R90-917886-1



# DEVELOPMENT OF DUAL FIBER REINFORCED GLASS MATRIX COMPOSITES FOR STRUCTURAL SPACE BASED APPLICATIONS



Prepared by

W. K. Tredway
K. M. Prewo

FINAL REPORT

Contract N00014-88-C-0251

for

Department of the Navy
Office of Naval Research
Arlington, VA 22217

May 31, 1990



UNITED TECHNOLOGIES RESEARCH CENTER
East Hartford, Connecticut 06108

UNITED
TECHNOLOGIES
RESEARCH
CENTER
East Hartford, Connecticut 06108

R90-917886-1

# Development of Dual Fiber Reinforced Glass Matrix Composites for Structural Space Based Applications

FINAL REPORT

Contract N00014-88-C-0251

**REPORTED BY** William K. Tredway

William K. Tredway

Karl M. Prewo

Karl M. Prewo

**APPROVED BY** Earl R. Thompson

Earl R. Thompson

**DATE** May 31, 1990

# TABLE OF CONTENTS





## SUMMARY

This report summarizes a program performed at United Technologies Research Center (UTRC) under SDIO/IST funding (through the Office of Naval Research) to create zero CTE glass matrix composites through a dual fiber reinforcement approach. This program was part of an overall effort at UTRC which is still ongoing to prepare fiber reinforced glass matrix composites for deployment in space as satellite primary structural materials. By combining high elastic modulus carbon fibers with boron or silicon carbide monofilaments in a glass matrix, it has been demonstrated that composites with specific stiffness (elastic modulus divided by density) and coefficient of thermal expansion (CTE) equivalent of superior to the best current metal matrix composites can be achieved. These attributes, combined with the high temperature stability and atomic oxygen resistance of glass matrix composites, make these materials particularly attractive for SDI applications requiring high performance, long term durability, and survivability.

# I. INTRODUCTION

Over the past several years, SDIO/IST (through ONR) have funded UTRC to develop high performance fiber reinforced glass matrix composites for use in space satellite applications. The carbon fiber reinforced glass matrix (C/Glass) composite system shows exceptional potential for SDI needs because it can provide a combination of high performance, high temperature capability, light weight, and ease of fabrication all in one system. This combination is unique when compared with the capabilities of any other potential candidate material systems including current polymer matrix, metal matrix, and carbon-carbon composites.

Specific tasks in the overall SDI program over the past several years have included the following:

- Development of a basic understanding of the fundamental mechanisms controlling the mechanical performance of C/Glass composites;
- Development of high modulus C/Glass composites using ultra-high modulus pitch-based carbon fibers;
- Development of C/Glass composites exhibiting a combination of high specific stiffness and near-zero thermal expansion;
- Increasing the temperature capability of C/Glass composites through the use of refractory glass and glass-ceramic matrix compositions;
- Development of advanced fabrication techniques which will facilitate the use of C/Glass composites in structural space-based applications;
- Participate in SDI-sponsored programs to build a data base for various C/Glass composite systems so that these materials can be considered by designers of space systems and hardware.

The herein described program has addressed the goal of creating high specific stiffness, zero CTE composites for structural applications in space by using a dual fiber reinforcement approach. In this effort, a variety of monofilaments with and without fiber coatings were added as a secondary reinforcement to pitch fiber reinforced borosilicate glasses. The results are presented herein with emphasis on the scientific aspects of composite tensile stress-strain performance, CTE behavior, and interface chemistry.

# II. BACKGROUND

Fiber reinforced glass matrix composites have been investigated over the past two decades due to their potential for high strength and stiffness, excellent toughness, low density, and fabricability [1-4]. United Technologies Research Center (UTRC) has been active in this area for many years, investigating the use of a variety of carbon, silicon carbide, and oxide fibers and yarns in a host of different glass and glass-ceramic matrices for many aerospace and industrial applications [4-10]. Carbon fiber reinforced glass matrix (C/Glass) composites have been the subject of much interest in recent years [9, 11-13] because of their potential to serve as structural materials in space-based applications (*e.g.*, satellite platforms). Their unique combination of low density, high strength and stiffness, good toughness, excellent dimensional stability, high temperature capability, and fabricability make these materials ideally suited for many such applications.

Materials to be used for the construction of space based satellites require many unique characteristics; however, two of the most critical requirements are high specific stiffness and near-zero thermal expansion [14]. Specific stiffness, which is the elastic modulus divided by the material density, needs to be high to provide stability and prevent oscillations during maneuvering of booms and other such structures. Near-zero thermal expansion behavior ($\pm 0.5 \times 10^{-6}$/°C) is necessary to maintain alignment of optics during orbit as the temperature fluctuates from -100°C to +70°C and also to minimize thermal fatigue associated with expansion and contraction during each orbit. It has previously been shown on a separate SDIO/ONR-funded program that unidirectionally reinforced C/Glass composites containing ultra-high modulus pitch-based carbon fiber can meet the high specific stiffness requirement while also providing strength in excess of 750 MPa [12]. The CTE of these composites, however, is somewhat more negative than $-0.5 \times 10^{-6}$/°C over the temperature range of -100°C to +70°C. One approach that would increase the CTE behavior into the desired range would be to change the unidirectional ply orientation to a multidirectional angle-ply layup. However, this approach would sacrifice a significant amount of the composite stiffness [9] and would still result in a composite with somewhat negative CTE behavior. The optimum situation would be to develop a means of increasing the composite CTE to near-zero over the desired temperature range while still maintaining the high specific stiffness of pitch-fiber reinforced glass matrix composites.

One concept for achieving this combination of properties that has been developed at UTRC involves the addition of a second unidirectional fiber reinforcement, possessing high stiffness and a positive CTE, to a unidirectional pitch fiber reinforced glass matrix composite. By adding the appropriate amount of this secondary reinforcement to the composite, the negative longitudinal thermal strain imparted by the pitch-based carbon fiber can be offset by the positive thermal strain of the secondary reinforcement, resulting in a composite exhibiting both near-zero CTE behavior and high stiffness. In this study, large diameter (100-144 μm) boron and SiC

monofilaments were chosen as this second fiber reinforcement. Both types of monofilament possess excellent mechanical properties and have demonstrated that they can be successfully used as the sole reinforcement for glass and glass-ceramic matrix composites [15-17]. The expected effect of adding both boron and SiC monofilaments to a borosilicate glass matrix composite reinforced with pitch-based carbon fiber is illustrated in Figure II-1 (the volume ratio of carbon fiber to glass is held constant at 40:60). These curves were calculated using the well-known "rule-of mixtures" equation for longitudinal composite modulus and the equation derived by Schapery [18] for composite thermal expansion. It can be seen that the effect on elastic modulus is minimal since the stiffness of the monofilaments is only slightly greater than that of the pitch-fiber glass composite. Composite thermal expansion, however, is seen to become more positive with the addition of monofilament, so that zero thermal expansion is achieved with ~20 vol% boron monofilament and ~28 vol% SiC monofilament.

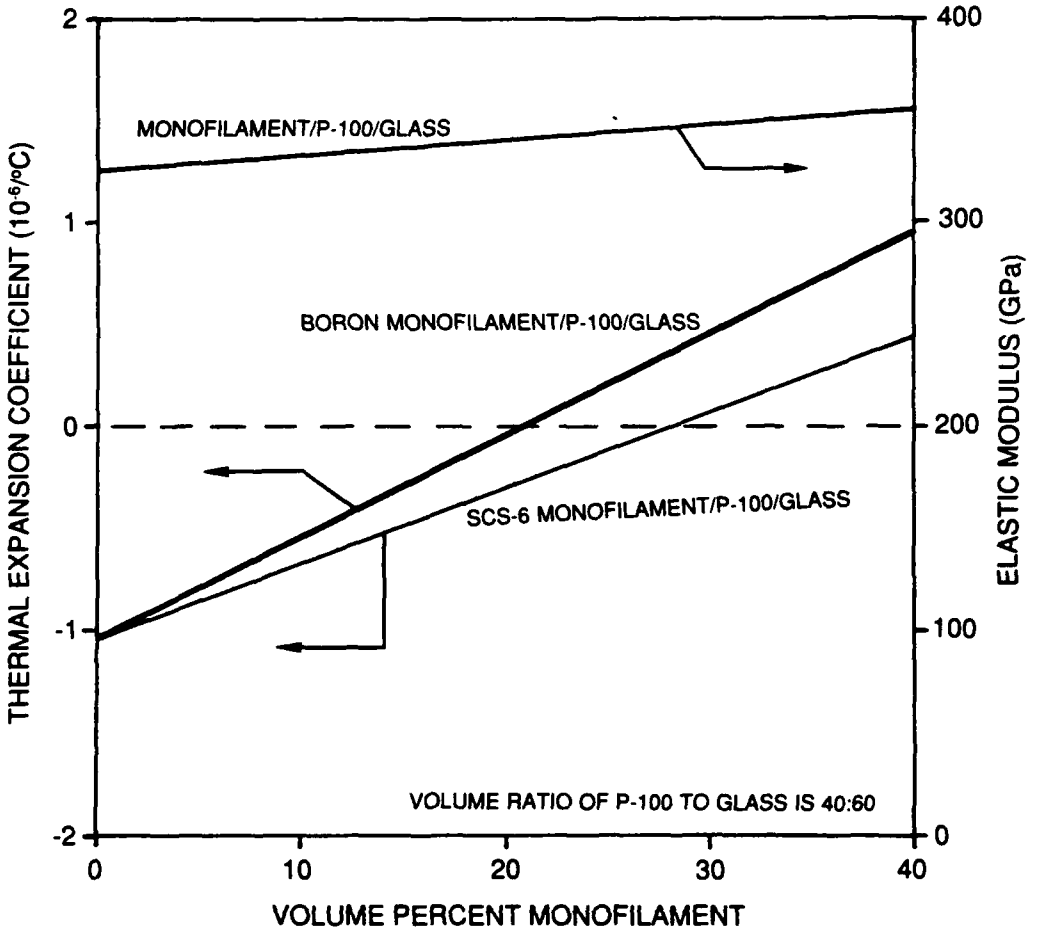


**Figure II-1. Calculated thermal expansion and elastic modulus of uniaxially dual fiber reinforced borosilicate glass matrix composites.**

90-5-78-17

# III. EXPERIMENTAL PROCEDURE

Uniaxially reinforced laminated composites containing the monofilaments and carbon fibers were prepared by hot-pressing. The matrix composition for all the composites was a commercially available borosilicate glass*. The pitch-based carbon fiber used as the primary reinforcement for all the composites was P-100**. Uncoated and coated monofilaments utilized as secondary reinforcements are listed in Table III-1. Properties of all the constituents are summarized in Table III-2. Typical fiber loadings were 20-25 volume % for the monofilaments and 30-35 volume % for the carbon fiber. Consolidation of the composites was achieved by hot-pressing in an inert atmosphere. This procedure resulted in nearly fully-densified composites containing 1-2 % porosity.

Composite thermal expansion in a direction parallel to the fibers was measured against a $SiO_2$ standard using a dilatometer.*** Samples were heated/cooled in an inert atmosphere over the thermal cycle of room temperature $\rightarrow$ +150°C $\rightarrow$ -150°C $\rightarrow$ room temperature at 2°C/min. At least two thermal cycles were always employed. Average coefficient of thermal expansion as a function of temperature was determined from the thermal strain data by taking the derivative of a 3rd order polynomial curve that was a least-squares fit to the data.

Tensile testing of the composites was performed using straight-sided specimens at a crosshead speed of 0.13 cm/min. In all cases the gage length was 2.54 cm. Composite strain was monitored using glued-on strain gages on both sides of the tensile specimen.

Fracture behavior was observed using both optical and scanning electron microscopy (SEM) techniques#. SEM samples were sputter-coated with gold to prevent charging in the microscope.

Composition analysis of the monofilament coatings in the as-received state as well as of the coating-matrix interfacial region after composite fabrication was performed using a scanning Auger multiprobe (SAM)##. For the interfacial analyses, composites were split interlaminarly (parallel to the monofilament/carbon fiber laminae) so that both a monofilament and a matrix trough (where a monofilament had pulled away during fracture) could be analyzed. In this manner, a composition profile of the interfacial region could be constructed.

---

* Code 7740, Corning Glass Works, Corning, NY

** Amoco Performance Products, Ridgefield, CT

*** Dilatronic 2, Theta Industries, Inc.

\# JSM-35, JEOL

\#\# PHI 600, Perkin-Elmer

**Table III-1 - Monofilaments Used as Composite Reinforcements**

| Monofilament | Coating | Trade Name | Manufacturer |
|---|---|---|---|
| Boron | --- | --- | Textron |
| Boron | $B_4C$ | --- | Textron |
| Boron | SiC | Borsic | United Technologies Corp. |
| Boron | SiC | Sicabo | Textron (monofilament)<br>Composites, Inc. (coating) |
| SiC | C/SiC | SCS-6 | Textron |

**Table III-2 Constituent Properties**

| Constituent | Density (g/cc) | Elastic Modulus (GPa) | Tensile Strength (MPa) | Room Temp. CTE ($10^{-6}$/°C) |
|---|---|---|---|---|
| 7740 Glass | 2.23 | 63 | --- | 3.2 |
| P-100 Fiber | 2.16 | 724 | 2240 | -1.6 |
| Boron | 2.49 | 400 | 3500 | 3.4 |
| Borsic | 2.49* | 400* | 3500* | 3.4* |
| Sicabo | 2.49* | 400* | 3500* | 3.4* |
| SCS-6 | 3.05 | 400 | 3500 | 2.25 |

* Assumed to be the same as that of boron

# IV. RESULTS AND DISCUSSION

In general, the microstructures of all the composites were similar, with fairly uniform distribution of the monofilaments throughout the matrix. The carbon fiber was also distributed uniformly throughout the matrix and in between the monofilaments (Figure IV-1). A few regions of isolated porosity were found in some of the composites, but they were not believed to be of any significance in terms of composite performance. The following sections describe results based on the type of monofilaments used for reinforcement. Reference is made to specific composite examples throughout the report; a comprehensive list of all composites fabricated is presented in the Appendix.

## IV.1. Uncoated Monofilaments

Uncoated boron monofilaments were initially used as the secondary reinforcement for three reasons: (1) boron has a high elastic modulus and a large positive CTE compared to carbon fiber; (2) uncoated boron monofilament had been used successfully in the past as the sole reinforcement for borosilicate glass matrix composites [15], and; (3) the cost and availability of the boron monofilament made it an attractive choice. The measured thermal expansion behavior of a composite containing a combination of boron monofilament and P-100 carbon fiber is shown in Figure IV-2(a). The CTE behavior of a P-100 reinforced glass composite is also included for comparison. It is clear that the addition of the boron monofilament has led to the predicted increase in composite CTE into the near-zero domain over the temperature range indicated. The thermal strain behavior of the carbon-plus-boron reinforced composite over the second thermal cycle is shown in Figure IV-2(b). The thermal strain exhibits a small amount of hysteresis behavior over the thermal cycle, which is also a characteristic that is commonly observed in C/Glass composites [12, 19]. The magnitude of the hysteresis is $5 \times 10^{-6}$ or less over the entire cycle, however, which is quite manageable from the aspect of dimensional stability.

The tensile stress-strain behavior of the composite containing uncoated boron monofilament is summarized in Table IV-1. A typical stress-strain curve for this composite is shown in Figure IV-3. The composite exhibits linear elastic behavior up to a strain level of approximately 0.02%, at which point the stress-strain behavior deviates somewhat from linearity. A similar type of non-linear stress-strain behavior is commonly observed in other C/Glass composite systems reinforced with pitch-based carbon fiber such as P-100 [12, 19]. Overall, the tensile performance of the composite was somewhat less than expected given the successful reinforcement of glass matrices with boron monofilaments which had been reported in the literature [15]. The initial elastic modulus of the composite (255 GPa) was less than expected, being ~73% of that predicted based on a simple rule-of-mixtures calculation. The

ultimate tensile strength and the failure strain of the composite were also quite low. Specific stiffness for this composite was reasonably high at $118 \times 10^7$ cm; however, this was still slightly below the range of other materials that are being considered for stiffness-critical space based applications [14]. Examination of the fracture surface of the composite indicated that the composite failed in a brittle manner, with no evidence of monofilament pullout (Figure IV-4). Close examination reveals that while some toughness was provided to the composite via pullout of the P-100 carbon fibers, the boron monofilaments appear to be bonded very strongly to the glass. It appears that the crack propagating through the matrix experienced no deflection at the monofilament-matrix interface, resulting in continued propagation directly through the boron monofilament.

Also evident in Figure IV-4 is degradation of the interface between the core of the monofilament (tungsten boride) and the boron monofilament itself (hereafter referred to as the core-mantle interface). This degradation has been reported previously in studies of the effect of thermal treatments on the properties of boron monofilaments [20, 21]. In these reported studies the degradation was found to correspond to massive void formation resulting from the diffusion of loosely bound boron atoms from the fiber interior to the surface to replace boron atoms removed from the surface due to oxidation. The diffusion of these boron atoms leads to the formation of vacancies which ultimately coalesce at the core-mantle interface to form visible voids. Although conditions varied, 800-900°C seems to be the temperature range above which diffusion and void formation occurred most rapidly. Another observation in these reported studies was that a substantial amount of fiber tensile strength was lost once interfacial void formation became very noticeable.

In the case of the glass matrix composites studied in the current investigation, it seems likely that boron diffused into the glass matrix during composite fabrication (1250°C maximum temperature), either as the result of oxidation of the boron or due to the gradient in boron concentration between the fiber and the glass. This boron diffusion then resulted not only in the void formation observed at the core/fiber interface, but also in strength and modulus degradation of the monofilament and a very strong interfacial bond between the boron monofilament and the glass matrix. This explains the rather poor tensile performance of the composite as well as the brittle nature of the fracture surface.

The reason for the discrepancy with the above referenced work [15] utilizing boron monofilament is believed to be related to the composite processing temperature. While the conditions for hot-pressing of these earlier composites were not stated explicitly, previous experience at UTRC has shown that monofilament reinforced glasses can be optimally fabricated at temperatures slightly greater than the softening temperature of the matrix, which is ~820°C for the glass used in the previously reported investigation. If the boron reinforced glass composite was fabricated in this temperature range (850-900°C), little if any fiber degradation would have resulted from void formation. However, for the present study, processing conditions were

determined by the presence of the carbon fiber yarn which requires higher consolidation temperatures to remove porosity from between these small diameter fibers.

## IV.2. Coated Monofilaments

Concern over the brittle fracture behavior resulting from the strong monofilament-matrix adhesion in the boron reinforced composites led to the use of coated monofilaments in the hope that the fiber coating would prevent outward diffusion of the boron into the glass, thereby limiting monofilament-matrix adhesion and improving composite fracture toughness and overall tensile performance. Several different coated monofilaments were utilized, as summarized in Table III-1. The different coating materials evaluated were $B_4C$, SiC, and a mixture of carbon and SiC. In all cases the surface coatings were applied by chemical vapor deposition.

### *IV. 2. 1. $B_4C$-Coated Boron Monofilament*

The thermal expansion behavior of the composite reinforced with $B_4C$-coated boron was intermediate between that of the two composites illustrated previously in Figure IV-2, i.e. somewhat less positive than the co..iposite containing uncoated boron. However, the CTE was still between $-0.7 \times 10^{-6}$ /°C and zero /°C over the temperature range of interest (see Figure IV-5). Composite thermal strain again exhibited closed-loop hysteresis behavior, with the magnitude of the hysteresis being $10\text{-}15 \times 10^{-6}$ over the entire thermal cycle.

The tensile performance of the composite reinforced with $B_4C$-coated boron monofilament is summarized in Table IV-1. The shape of the stress-strain curve (Figure IV-6) as well as the overall tensile performance was similar to that of the uncoated boron composite discussed previously. Composite modulus was only about 70% of that expected based on a rule-of-mixtures calculation. The $B_4C$ coating did not improve tensile strength, with failure strain also being low. The fracture behavior of the composite was not quite as brittle as that seen with the uncoated boron monofilaments, however, with the fracture surface exhibiting slight pullout of the $B_4C$-coated monofilaments (Figure IV-7). This suggests that the $B_4C$ coating was somewhat effective at preventing as strong an interfacial bond as that seen between the uncoated boron monofilament and the glass matrix.

The core-mantle interface again showed some signs of void formation [Figure IV-7(b)], although not to the same extent as seen in the uncoated boron monofilaments. Apparently the $B_4C$ coating did not act as an effective diffusion barrier for boron, allowing loosely bound boron atoms to migrate through to the glass matrix (diffusion of boron through $B_4C$ has been observed previously [22]). The formation of voids at the core-mantle interface again led to a degradation in monofilament performance which resulted in low composite tensile strength, modulus, and failure strain.

### *IV. 2. 2. SiC-Coated Boron and C/SiC-Coated SiC Monofilaments*

Composites reinforced with the SiC-coated boron (Borsic, Sicabo) and the C/SiC-coated SiC (SCS-6) were all superior to those described above. They all displayed similar characteristics with respect to thermal expansion, tensile stress-strain, and fracture behavior. They will therefore all be discussed together in this section. One noticeable difference between the Borsic and Sicabo reinforced composites and the SCS-6 reinforced composite, however, was their overall structural integrity. The Borsic and Sicabo reinforced composites sometimes tended to delaminate slightly or "fray" somewhat when machined into tensile and thermal expansion samples. This fraying always occurred between the monofilaments and the matrix and appeared to be associated with a weak interfacial bond. The SCS-6 reinforced composites, on the other hand, exhibited no such behavior.

The thermal expansion behavior of the composites containing Borsic, Sicabo, and SCS-6 differed somewhat from that seen in the boron and the $B_4C$-coated boron reinforced composites with respect to both the shape of the thermal strain curve and the magnitude of the CTE. In all cases, the measured CTE was close to that predicted at room temperature and fell within the near-zero domain from -100°C to +70°C, which corresponds to the range of temperatures experienced during an orbit in space.. Figure IV-8 illustrates this behavior for the Borsic reinforced composite (the behavior of the Sicabo reinforced composite is nearly identical). It can be seen that the thermal strain of the Borsic composite [Figure IV-8(b)] is more positive from room temperature to +150°C and less negative from room temperature to -150°C than the composite reinforced with uncoated boron [Figure IV-2(b)]. Since both composites contain approximately the same volume percent of monofilament and P-100 carbon fiber, this suggests that the Borsic monofilament is exerting more of an influence on composite thermal expansion than the uncoated boron. Because the CTE of both fibers should be essentially the same, the implication is that the in situ elastic modulus of the Borsic fiber is greater than that of the uncoated boron (based on the Schapery equation for composite CTE [18]). The thermal expansion behavior of the SCS-6 reinforced composite is shown in Figure IV-9. Both the thermal strain and the CTE characteristics are very similar to those exhibited by the Borsic and Sicabo reinforced composites with the exceptions that the CTE is slightly lower for the SCS-6 reinforced composite and that the thermal strain hysteresis displays a positive offset of approximately 15 x $10^{-6}$ between the beginning and end of the thermal cycle. The lower composite CTE is simply a reflection of the lower CTE of the SCS-6 monofilament compared to Borsic and Sicabo. The reason for the hysteresis in this particular composite system is not entirely understood.

The tensile performance of the composites reinforced with the Borsic, Sicabo, and SCS-6 monofilaments is summarized in Table IV-1. When compared with the use of boron, all three of these coated monofilaments resulted in significantly enhanced composite tensile performance, with high tensile strengths, increased failure strains, and substantial amounts of monofilament pullout. The SCS-6 reinforced composite exhibited especially high tensile strength, with 93%

translation of the monofilament strength to the composite. Figure IV-10 gives a macroscopic comparison of the difference in monofilament pullout between composites reinforced with boron and with Sicabo. Composites reinforced with Borsic and SCS-6 showed similar pullout behavior. (The shape of the tensile stress-strain curves of the composites reinforced with Borsic, Sicabo, and SCS-6 all exhibited very unusual behavior. This behavior will be discussed in detail in section IV. 2. 4.)

Figure IV-11 shows SEM micrographs of the fracture morphology demonstrated by the Sicabo reinforced composite. It is apparent from Figure IV-11(a) that the SiC coating is still intact on the boron monofilament. Figure IV-12 clearly indicates that there was no degradation of the core-mantle interface in a Borsic monofilament during fabrication, suggesting that the SiC coating prevented the diffusion of boron from the monofilament surface into the glass matrix. This lack of void formation resulted in retention of monofilament strength and stiffness during fabrication, which explains the improved tensile performance of the Borsic and Sicabo reinforced composites (relative to uncoated boron) as well as the higher monofilament elastic modulus suggested by the thermal expansion behavior described previously. It is evident from Figure IV-11(b) that fracture and debonding occurred between the coating and the matrix in the Sicabo reinforced composites, rather than within the coating or between the coating and the monofilament. Similar fracture behavior was also observed in the Borsic and SCS-6 reinforced composites.

### *IV. 2. 3. Auger Analysis*

Auger analysis was performed on the coating-matrix interfacial regions of the Borsic, Sicabo, and SCS-6 reinforced composites to establish the chemical composition across the interface. This procedure has been used extensively at UTRC in recent years in the analysis of interfacial chemistry in NICALON™ SiC yarn reinforced glass-ceramics with considerable success [8]. Figures IV-13(b) and IV-14(b) show the interfacial composition profile obtained from the Sicabo reinforced composite and the SCS-6 reinforced composite, respectively (the Auger profile obtained from the Borsic reinforced composite was very much similar to that shown in Figure IV-13(b)). It is evident from these profiles that a thin carbon-rich layer (~500-750Å thick) exists between the matrix and the fiber coating. Also present between the carbon layer and the coating is a region containing significant levels of silicon, oxygen, and carbon, with small amounts of boron and sodium that have diffused in from the matrix. The Si:O ratio suggests that $SiO_2$ may exist in this region (attempts to verify the existence of $SiO_2$ in the interfacial region using TEM techniques were unsuccessful due to instability of the material in the electron beam). Based on the location of the interface in all of the Auger profiles, it appears that fracture and debonding occurred *within* the carbon-rich layer in these composites, rather than between the carbon-rich layer and either the matrix or the coating. It is believed that this carbon-rich layer was also responsible in large part for the extensive monofilament pullout observed in these composites.

Auger analysis of the as-received Sicabo and Borsic monofilaments indicated that they contained ~53-57 at% carbon and ~43-47 at% silicon in the interior of the coating, with small amounts of oxygen (8-10 at%) very near the coating surface. Figure IV-13(a) shows the analysis of the SiC coating on the Sicabo monofilament. The amounts of silicon and carbon were relatively constant throughout the coating thickness. The analysis indicates that the coating is not stoichiometric SiC, but rather a carbon-rich SiC (this is in general agreement with recently reported work on Sicabo and Borsic fibers [23], with the exception that in that study both fibers were found to be nearly pure carbon at the coating surface.) The coating on the SCS-6 monofilament is also a mixture of carbon and SiC, though much richer in carbon than the coating on the Borsic and Sicabo monofilaments [Figure IV-14(a)]. It is proposed here that the carbon layer formation in the composites reinforced with the Borsic, Sicabo, and SCS-6 monofilaments is the result of a solid-state reaction between the SiC in the coating and oxygen from the glass and the fiber surface. This reaction was first described by Cooper and Chyung [24] in an investigation of carbon layer formation at the fiber-matrix interface in NICALON™ SiC yarn reinforced glass-ceramics, and can be given as [24]

$$SiC(s) + O_2(g) \rightarrow SiO_2(s) + C(s) \qquad (1)$$

The $SiO_2$ interlayer that forms between the carbon layer and the SiC coating can also be explained as being a product of the reaction described in equation (1). Of all the chemical equilibria pertaining to the oxidation of SiC, equation (1) has been determined to have the most negative Gibbs free energy and the most rapid reaction kinetics since it does not require the diffusion of gaseous reaction products away from the interface [24]. It seems reasonable, then, that this equation would most accurately explain the oxidation mechanism operative at the coating-matrix interface within these composites.

It has been suggested that the interfacial carbon layer that forms in NICALON™ reinforced glass-ceramic matrix composites consists not only of the carbon that forms from the reaction described by equation (1), but also is made up of the free condensed carbon that is inherently a part of the fiber [24]. This seems very plausible in light of additional observations made in SiC whisker reinforced composites [25] where it was found that interfacial carbon layer formation was much more prevalent in composites containing SiC whiskers that were nonstoichiometric (carbon-rich) than in composites reinforced with very pure, stoichiometric SiC whiskers. This corresponds well with the observations made in this investigation, since all of the monofilament coatings were found to be carbon-rich rather than stoichiometric SiC. In light of all these observations, it seems reasonable to conclude that the formation of the carbon layer at the interface between SiC and the glass matrix is enhanced significantly by the presence of excess condensed carbon in the SiC.

The monofilament-matrix interfacial region in the $B_4C$-coated boron reinforced composite was also analyzed via Auger analysis to determine its chemical composition. The analysis

revealed that a carbon-rich layer ~500-1000Å thick also existed between the coating and the matrix in this composite [Figure IV-15(b)]. This result was rather surprising in light of the almost complete lack of monofilament pullout observed during fracture of this composite. Analysis of the as-received fiber indicated that the coating was slightly carbon-rich $B_4C$ (approximately $B_{3.5}C$) in the interior of the coating, with a very thin region near the surface of the fiber (< 50Å) that was enriched in carbon and a small amount of oxygen [Figure IV-15(a)]. It is believed that strong bonding produced by the diffusion of boron through the $B_4C$ into the matrix almost completely offset the weak bond that would be expected from the formation of the carbon layer at the interface.

*IV. 2. 4. Tensile Stress-Strain Behavior of SCS-6, Borsic, and Sicabo Reinforced Composites*

As mentioned previously, the tensile stress-strain curves for the SCS-6, Borsic, and Sicabo reinforced composites all exhibited rather unusual behavior. The tensile stress-strain curve for the composite containing SCS-6 monofilament is illustrated in Figure IV-16. The curve starts out with an initial linear region where the elastic modulus is significantly less than the theoretical rule-of -mixtures modulus. The curve then deviates from linearity as the composite experiences a decrease in modulus. These first two sections of the curve closely resemble the stress -strain behavior of P-100 reinforced glass matrix composites [12, 19]. With increasing strain, the composite then exhibits an increase in stiffness and eventually enters a secondary linear region where the elastic modulus is greater than the initial stiffness.

The characteristics displayed in the latter portion of the curve prompted the use of cyclic tensile testing in an attempt to understand the mechanism(s) responsible for this unusual behavior (Figure IV-17). In the first two cycles, the composite was loaded to a strain level of 0.14%, which corresponded to the intermediate domain between the two linear regions of the stress-strain curve. The same initial composite stiffness was observed in these two cycles, indicating that the deviation from linearity did not correspond to permanent damage accumulation in the composite. In cycles 3 to 10, the composite was loaded to a strain level of 0.21%, which was well into the secondary linear region of the stress-strain curve. Here again the stiffness of the composite in the two linear regions was identical for every cycle, indicating that apparently no damage was being accumulated in the composite even on repeated loading to strain levels within 80% of the failure strain. The composite was then loaded to failure on the eleventh cycle.

One possible explanation for this stress-strain behavior that is suggested by the cyclic testing relates to the weak interfacial bond caused by the carbon-rich layer between the monofilaments and the glass matrix. Because of this weak bond, the monofilaments essentially do not contribute to the composite stiffness in the initial stages of loading, which effectively results in the composite acting as a P-100/Glass composite at low levels of strain. With increasing strain, however, the matrix begins to clamp around the monofilaments more tightly due to Poisson contraction effects, causing the composite stiffness to gradually begin increasing

around 0.10% strain. The clamping continues to increase the bonding until the monofilaments eventually contribute fully to the composite stiffness, which corresponds to the secondary linear region. On unloading, the process is simply reversed.

This argument is supported by considering the individual contributions that each constituent of the composite makes to the overall elastic modulus. Table IV-2 shows the theoretical contribution that the monofilament, carbon fiber, and glass matrix should each make to composite modulus based on a rule-of-mixtures calculation. The total theoretical composite stiffness based on these calculations is 335 GPa. The measured elastic moduli for the initial and secondary linear regions were 227 GPa and 296 GPa, respectively. As shown in Table IV-2, the measured stiffness in the initial region corresponds closely to the contribution made solely by the P-100 carbon fiber, while the measured modulus in the secondary region corresponds to the combined contributions of the carbon fiber and the SCS-6 monofilament. This suggests that the matrix does not contribute at all to the composite stiffness, which is a somewhat surprising implication. However, the severe thermomechanical stresses which the matrix is undoubtedly exposed to due to the thermal expansion differences of the constituents could result in severe matrix microcracking. The loss of the matrix contribution to composite stiffness during tensile testing of carbon fiber reinforced glass has been observed previously [9] and was attributed in that case to severe matrix microcracking and fiber-matrix debonding. In any case, this argument serves as only one possible explanation for the stress-strain behavior observed in the SCS-6 reinforced composite.

Tensile stress-strain curves for the Borsic and Sicabo reinforced composites are shown in Figures IV-18 and IV-19, respectively. The behavior of these composites is similar to that of the SCS-6 composite in the general shape of the curve and in the sense that the initial modulus corresponds closely to the contribution of the P-100 fibers alone (refer to Table IV-3). However, there is also a significant difference between the stress-strain behavior of the Borsic and Sicabo reinforced composites and the SCS-6 reinforced composite. This difference concerns the magnitude of the elastic modulus in the secondary linear region (refer to Table IV-3). For the Sicabo reinforced composite, the measured secondary modulus (214 GPa) is again greater than the initial modulus (193 GPa), but the magnitude is significantly below that predicted (316 GPa) using the argument presented for the SCS-6 reinforced composite. The secondary modulus for the Borsic reinforced composite (117 GPa) is not only less than that predicted using the SCS argument (294 GPa), but is also significantly less than the initial modulus (198 GPa).

While this difference in stress-strain behavior with respect to the magnitude of the secondary elastic modulus is not completely understood, it is believed to be related to differences in the nature of the coating-matrix interface in the various composite systems. As mentioned previously, it was believed that the interface between the Borsic and Sicabo monofilaments and the glass matrix was very weak based on observations of poor composite integrity in numerous samples following machining. The secondary elastic modulus behavior in these composites could be influenced by this extremely weak monofilament-matrix interfacial bond. One factor

which may contribute to a weaker bond in the Borsic and Sicabo reinforced composite systems relative to the SCS-6 reinforced composite system is the slightly greater CTE of these fibers relative to SCS-6. While transverse CTE data for the fibers is not readily available, the longitudinal CTE of boron monofilament is about 50% higher than that of SCS-6. If it can be assumed that transverse and longitudinal CTE reflect the same trends and that the CTE of Borsic and Sicabo is basically the same as that of boron, then it follows that the transverse CTE of these fibers should be higher than that of SCS-6. This higher transverse CTE would lead to a slightly larger "gap" between the coating and the matrix in the Borsic and Sicabo composites, which could prevent the matrix from ever fully clamping around the monofilaments during the Poisson contraction.

**Table IV-1 - Tensile Performance of Monofilament/P-100 Reinforced Glasses**

| Monofilament | Fiber Vol % | UTS (MPa) | Initial Modulus (GPa) | Theoretical Modulus (GPa) | Failure Strain (%) | Monofilament Fracture Morphology |
|---|---|---|---|---|---|---|
| Boron | 22 | 287 | 255 | 350 | 0.13 | Brittle |
| $B_4C$/Boron | 20 | 220 | 225 | 322 | 0.13 | Slight pullout |
| Borsic | 21 | 413 | 198 | 325 | 0.38 | Fibrous |
| Sicabo | 23 | 524 | 193 | 344 | 0.36 | Fibrous |
| SCS-6 | 20 | 655 | 227 | 335 | 0.27 | Fibrous |

**Table IV-2 - Modulus Contribution of Composite Constituents for the SCS-6 Reinforced Composite**

| Constituent | Fiber Vol % | Constituent Modulus (GPa) | Theoretical Contribution to Composite Modulus (GPa) | Theoretical Initial Modulus (GPa) | Theoretical Secondary Modulus (GPa) |
|---|---|---|---|---|---|
| SCS-6 Monofilament | 20 | 400 | 80 | | 80 |
| Carbon Fiber | 31 | 723 | 224 | 224 | 224 |
| Glass Matrix | 49 | 63 | 31 | ___ | ___ |
| | | | 335 | 224 | 304 |
| | | | *Measured Modulus* | 227 | 296 |

**Table IV-3 - Modulus Contribution of Composite Constituents for the Sicabo and Borsic Reinforced Composites**

| Constituent | Fiber Vol % | Constituent Modulus (GPa) | Theoretical Contribution to Composite Modulus (GPa) | Theoretical Initial Modulus (GPa) | Theoretical Secondary Modulus (GPa) |
|---|---|---|---|---|---|
| Sicabo Monofilament | 23 | 400 | 92 | | 92 |
| Carbon Fiber | 31 | 723 | 224 | 224 | 224 |
| Glass Matrix | 44 | 63 | 28 | ___ | ___ |
| | | | 344 | 224 | 316 |
| | | | *Measured Modulus* | 193 | 214 |

| Constituent | Fiber Vol % | Constituent Modulus (GPa) | Theoretical Contribution to Composite Modulus (GPa) | Theoretical Initial Modulus (GPa) | Theoretical Secondary Modulus (GPa) |
|---|---|---|---|---|---|
| Borsic Monofilament | 21 | 400 | 84 | | 84 |
| Carbon Fiber | 29 | 723 | 210 | 210 | 210 |
| Glass Matrix | 49 | 63 | 31 | ___ | ___ |
| | | | 325 | 210 | 294 |
| | | | *Measured Modulus* | 198 | 117 |

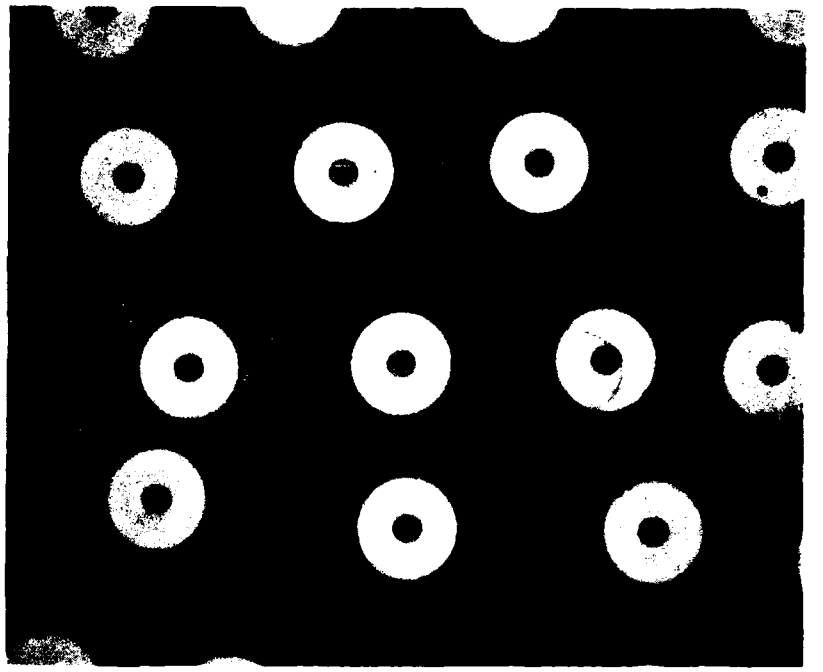

(a)

200μm

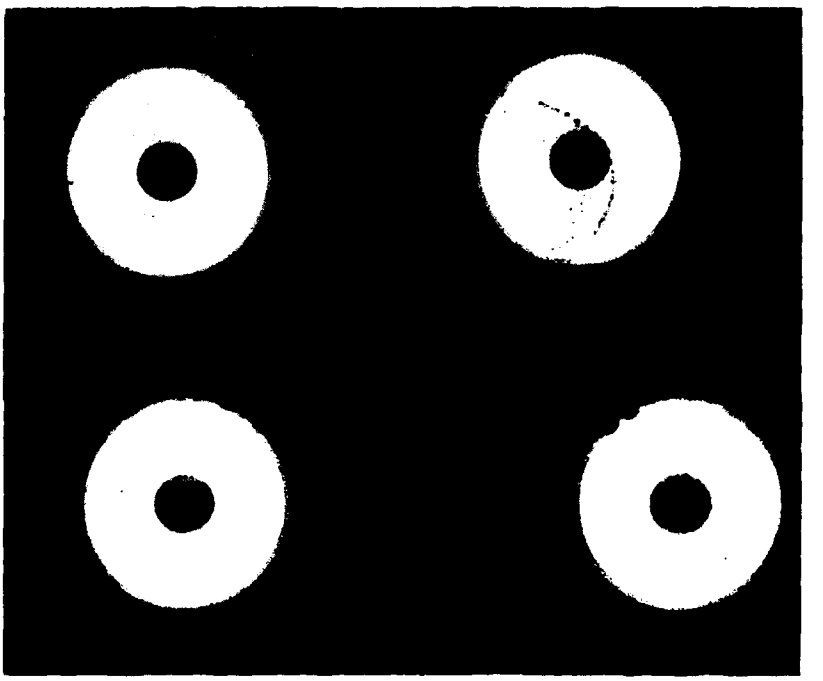

(b)

100μm

**Figure IV-1. Microstructure of dual fiber reinforced borosilicate glass matrix composites.**

90-5-78-16

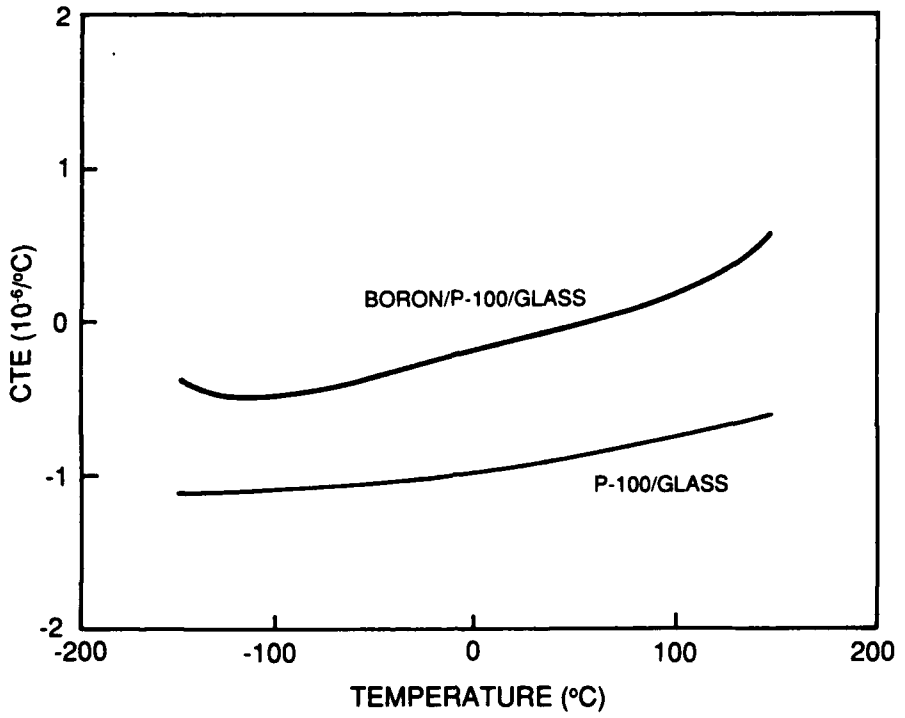


**Figure IV-2 (a). Thermal expansion coefficient vs temperature for a boron monofilament/ P-100/glass composite and for a P-100/glass composite.**

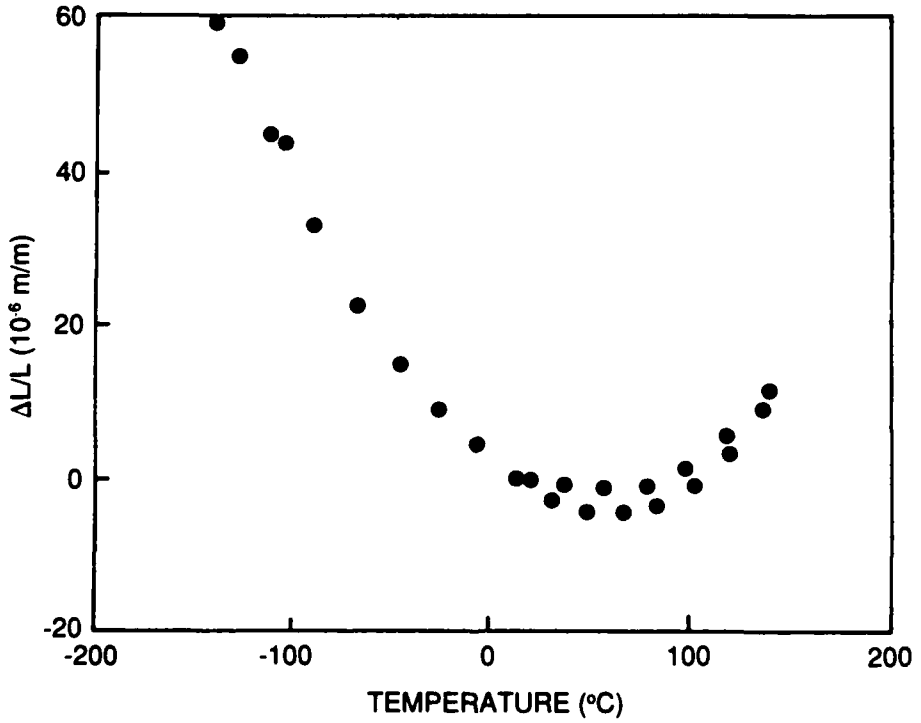


**Figure IV-2 (b). Thermal strain vs temperature for a boron monofilament/P-100/glass composite.**

90-5-78-15

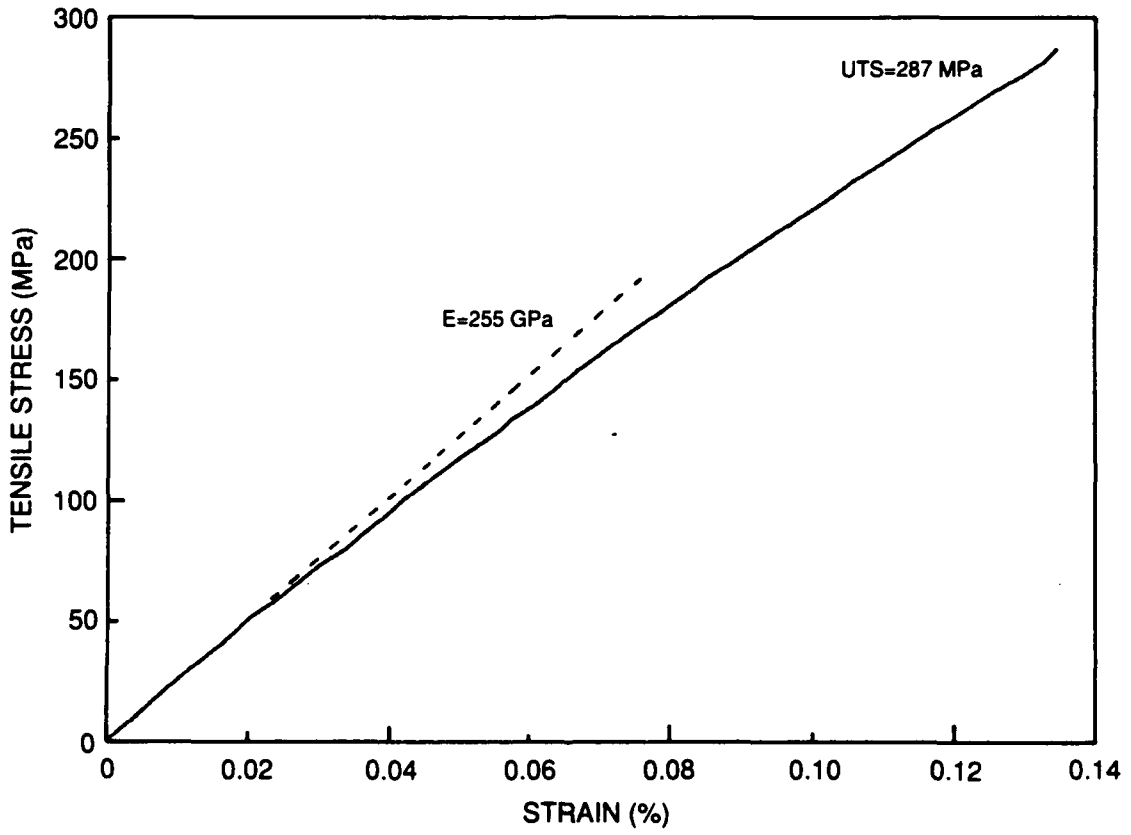


**Figure IV-3. Tensile stress-strain behavior of a uniaxially reinforced boron monofilament/ P-100/glass composite.**

90-5-78-14


**Figure IV-4. Tensile fracture surface of a boron monofilament/P-100/glass composite.**

90-5-78-13

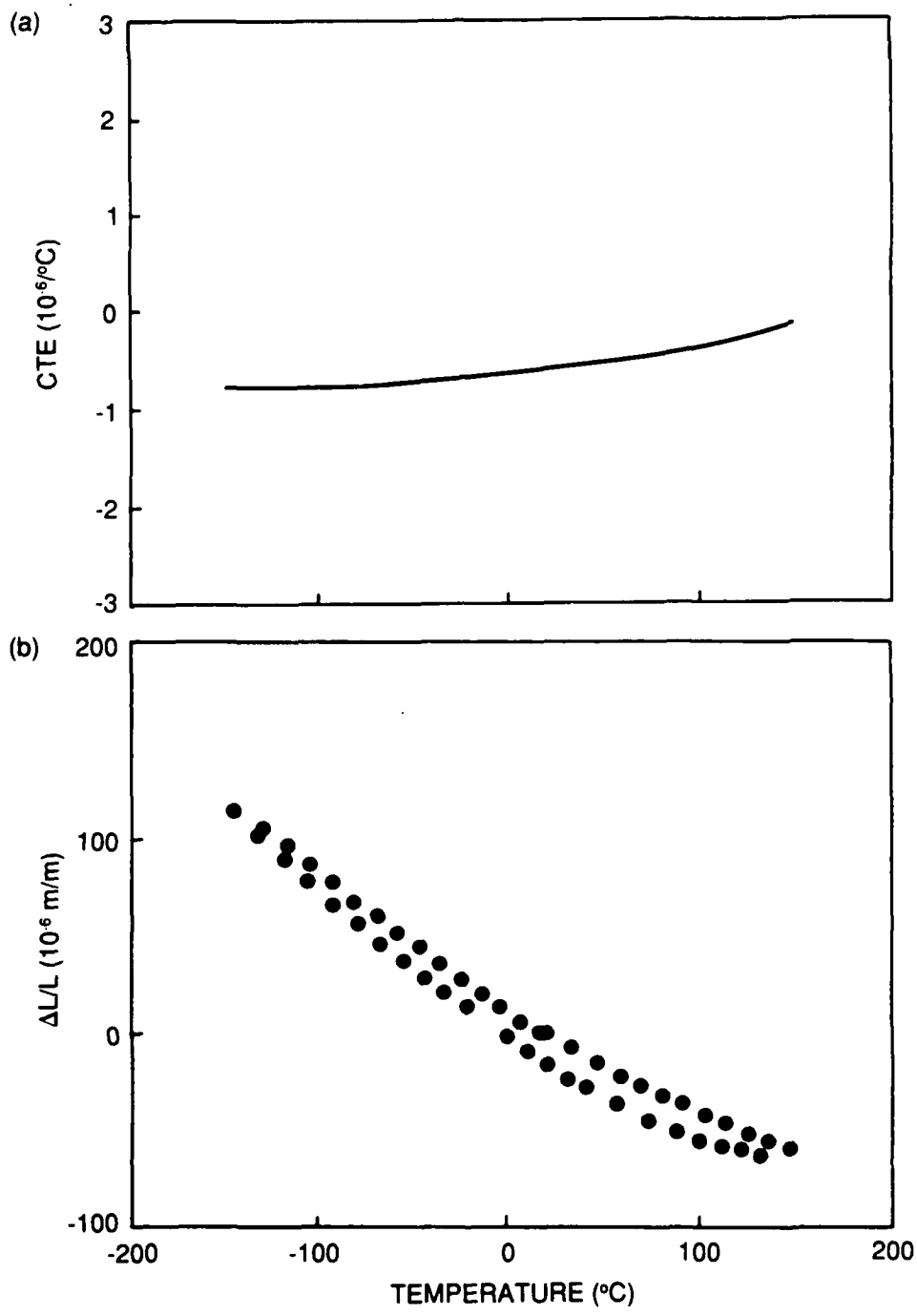


**Figure IV-5. (a) thermal expansion coefficient and (b) thermal strain vs temperature for a $B_4C$-coated boron/P-100/glass composite.**

90-5-78-1

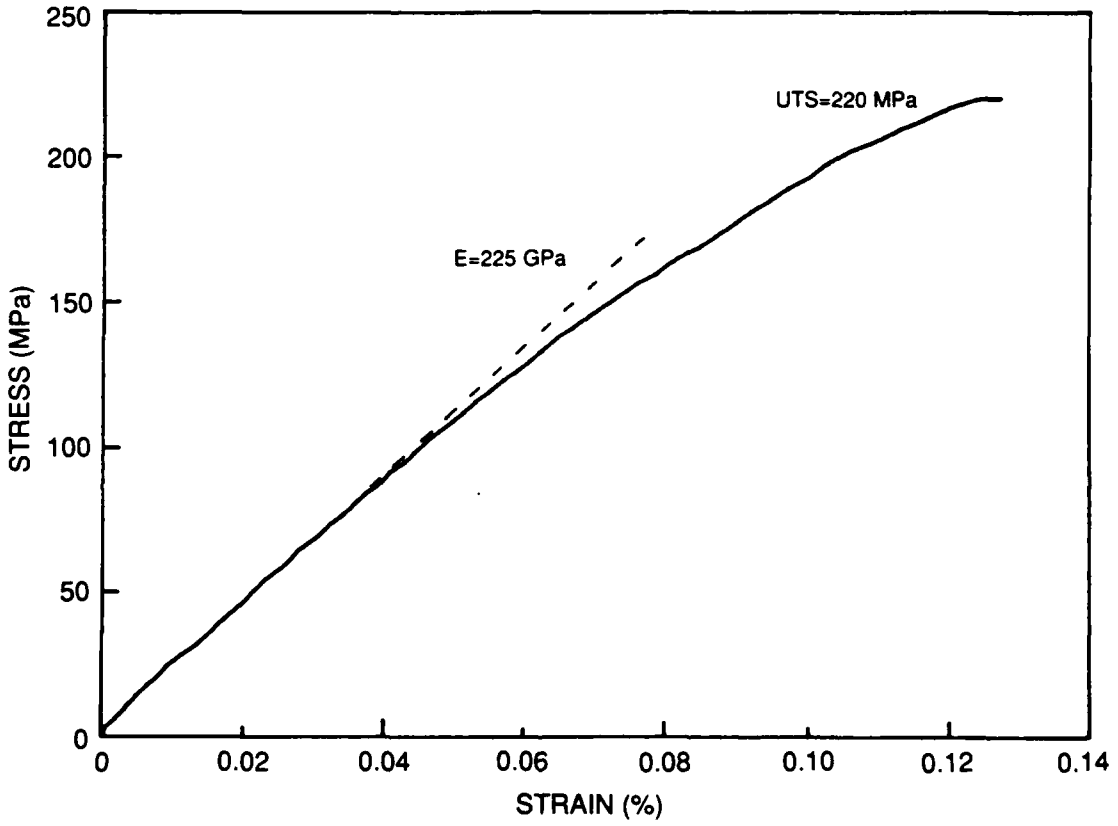


**Figure IV-6. Tensile stress-strain behavior of a uniaxially reinforced $B_4C$-coated boron/ P-100/glass composite.**

90-5-78-18

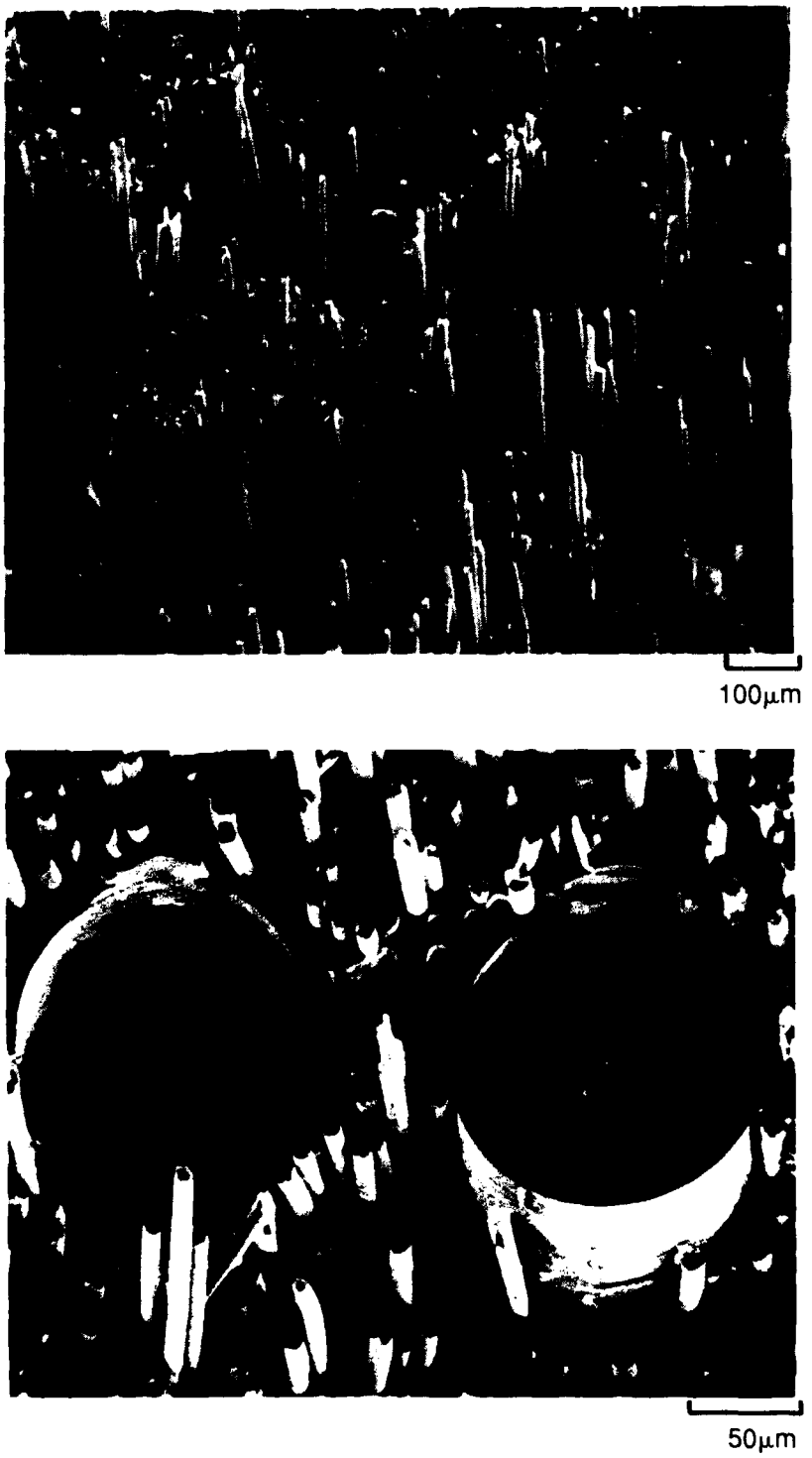


**Figure IV-7. Tensile fracture surface of a $B_4C$-coated boron/P-100/glass composite. Degradation of the core/mantle interface is evident in (b).**

90-5-78-7

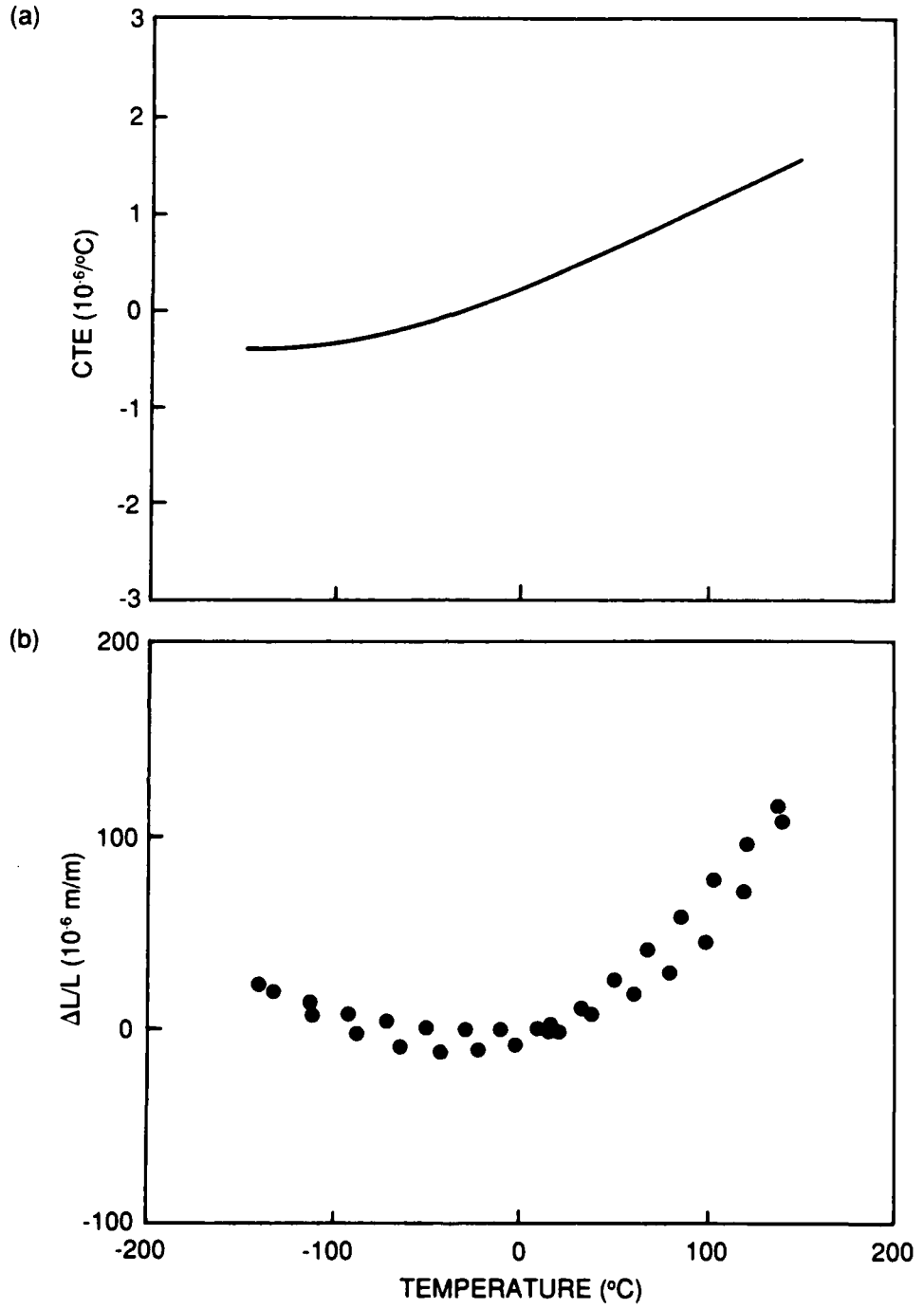


**Figure IV-8. (a) Thermal expansion coefficient and (b) thermal strain vs temperature for a Borsic/P-100/glass composite.**

90-5-78-12

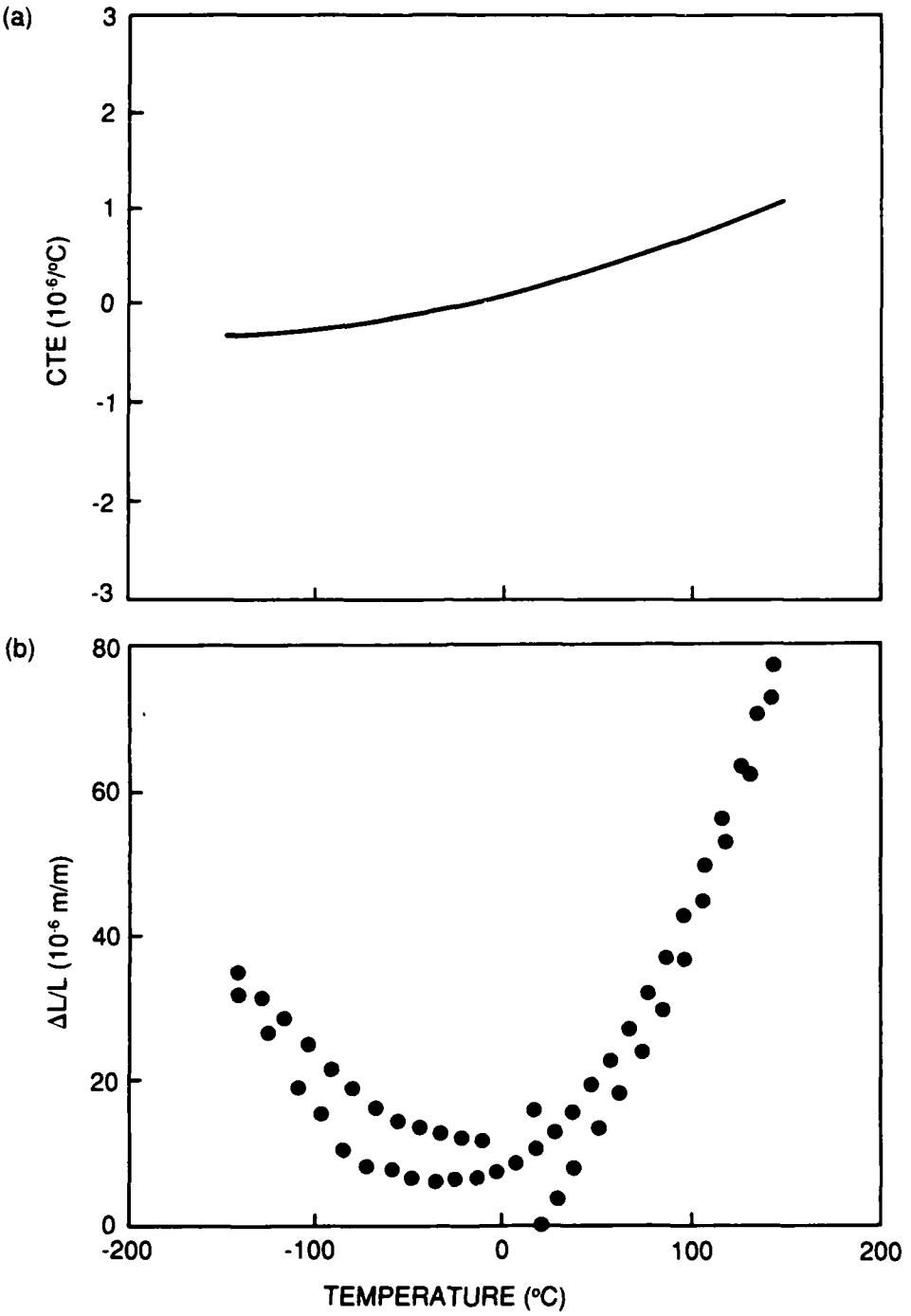


**Figure IV-9. (a) Thermal expansion coefficient and (b) thermal strain vs temperature for a SCS-6/P-100/glass composite.**

90-5-78-2

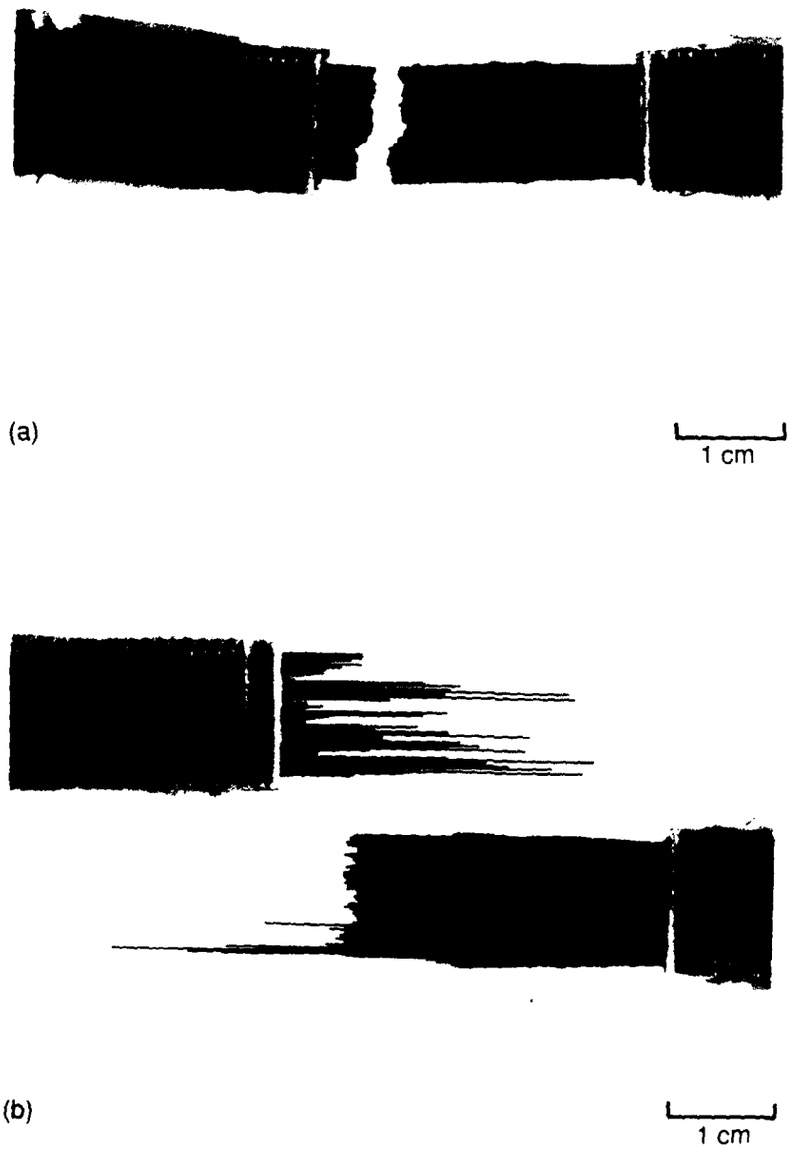


**Figure IV-10. Fractured tensile samples of (a) a boron/P-100/glass composite and (b) a Sicabo/ P-100/glass composite showing the difference in monofilament pullout length.**

90-5-78-11

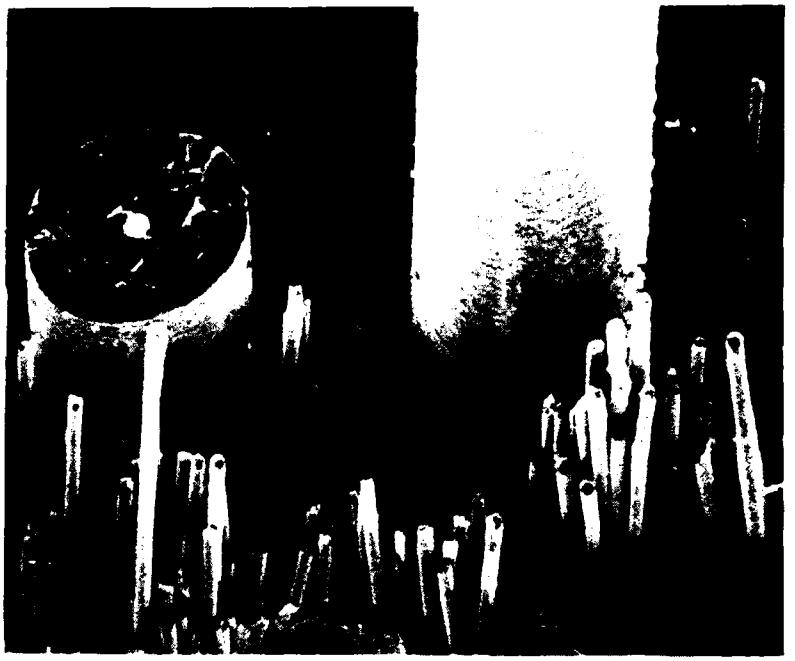


**Figure IV-11. Tensile fracture surface of a Sicabo/P-100/glass composite. (a) The SiC coating is still intact on the monofilaments after fracture. (b) Debonding is evident between the SiC coating and the matrix.**

90-5-78-10

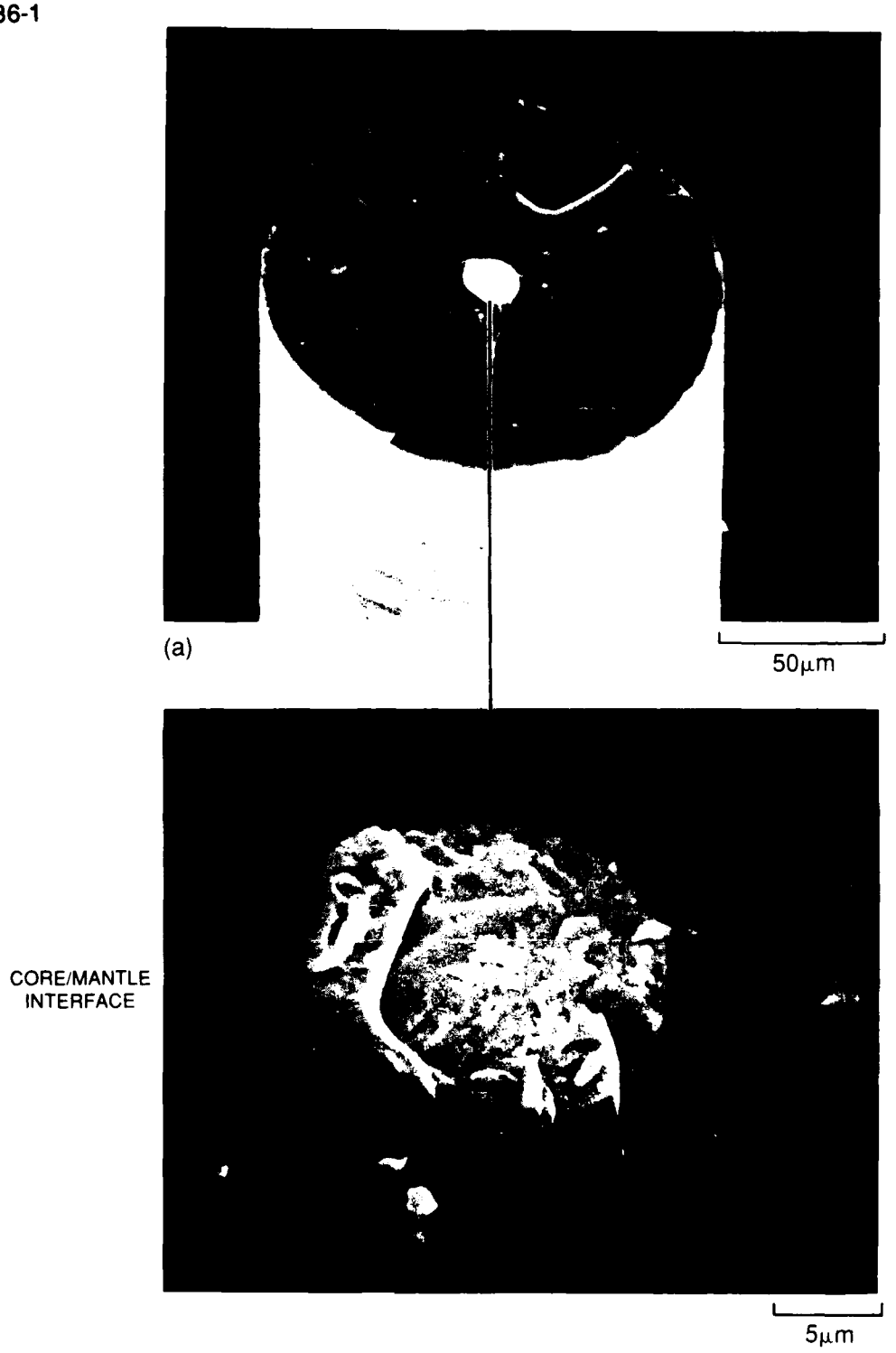


**Figure IV-12. Borsic monofilament from a tensile fracture surface showing no degradation at core/mantle interface.**

90-5-78-6

R90-917886-1

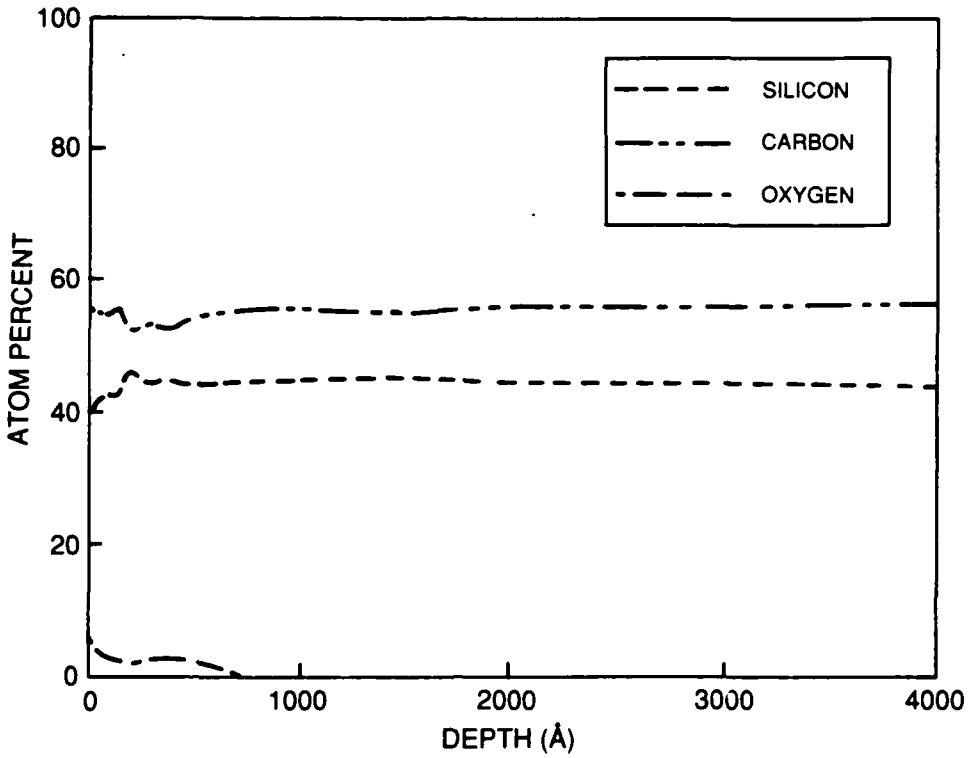


**Figure IV-13 (a). Auger analysis of the SiC coating on Sicabo monofilament.**

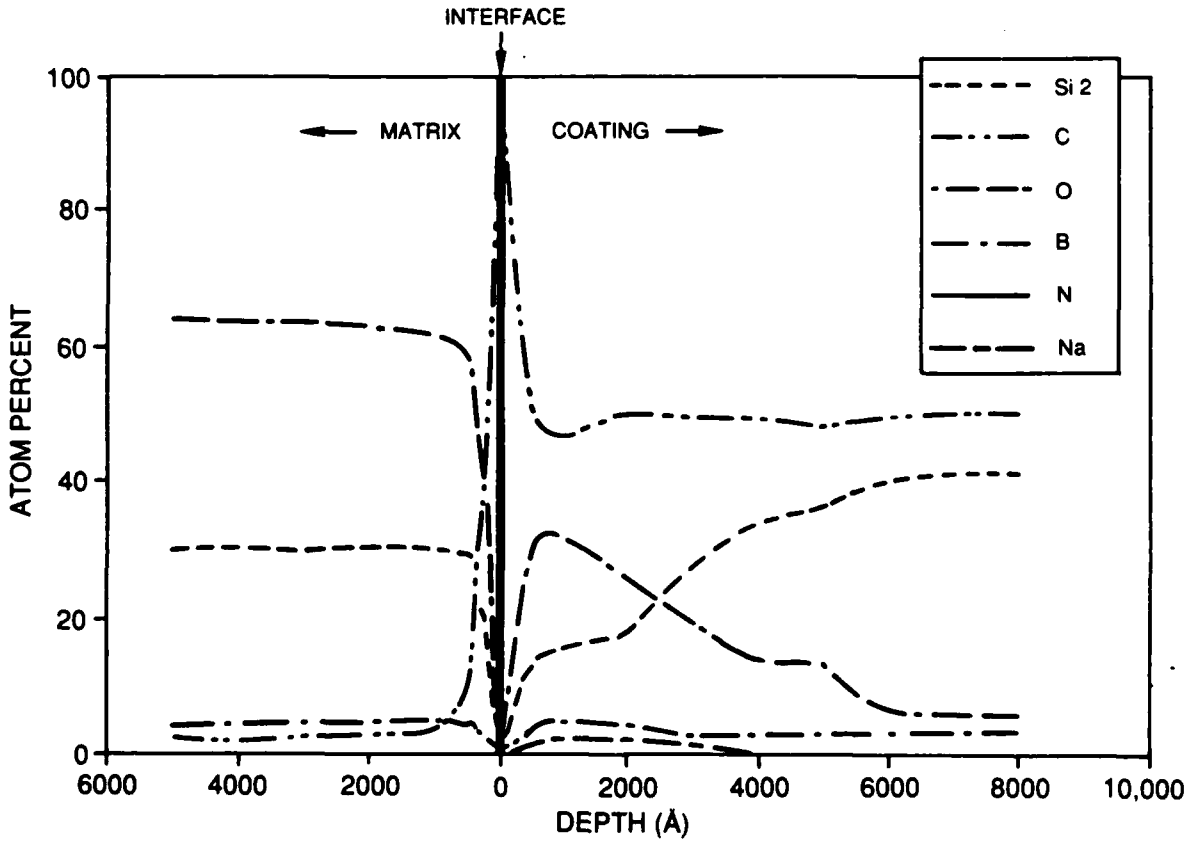


**Figure IV-13 (b). Auger analysis of the coating-matrix interface in a Sicabo/P-100/glass composite.**

90-5-78-4

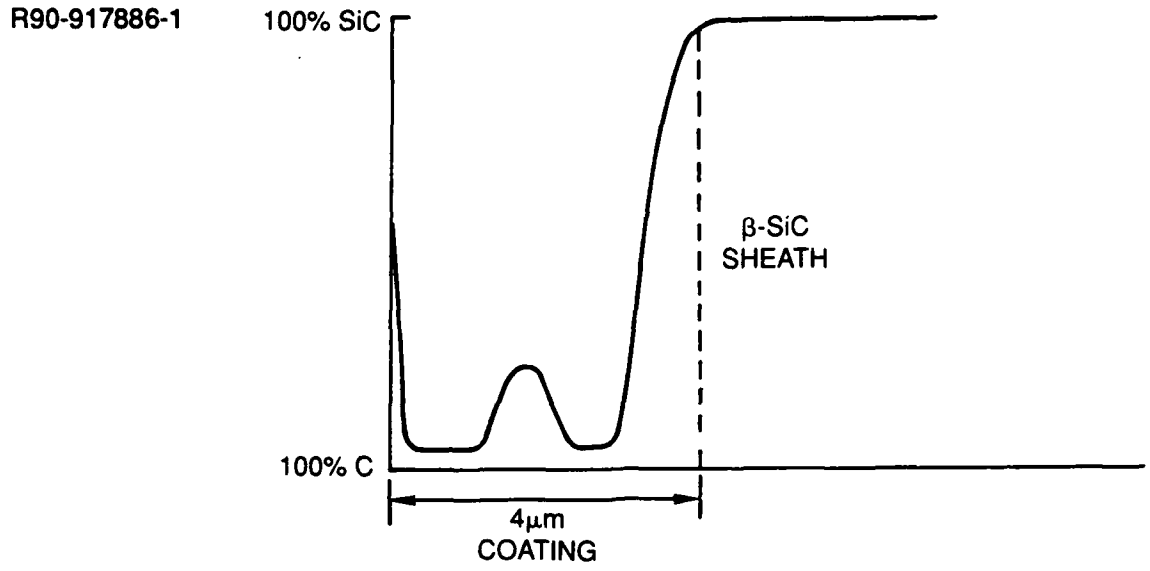


**Figure IV-14 (a). Schematic composition profile of the coating on an SCS-6 monofilament (courtesy of J. DiCarlo, NASA-Lewis).**

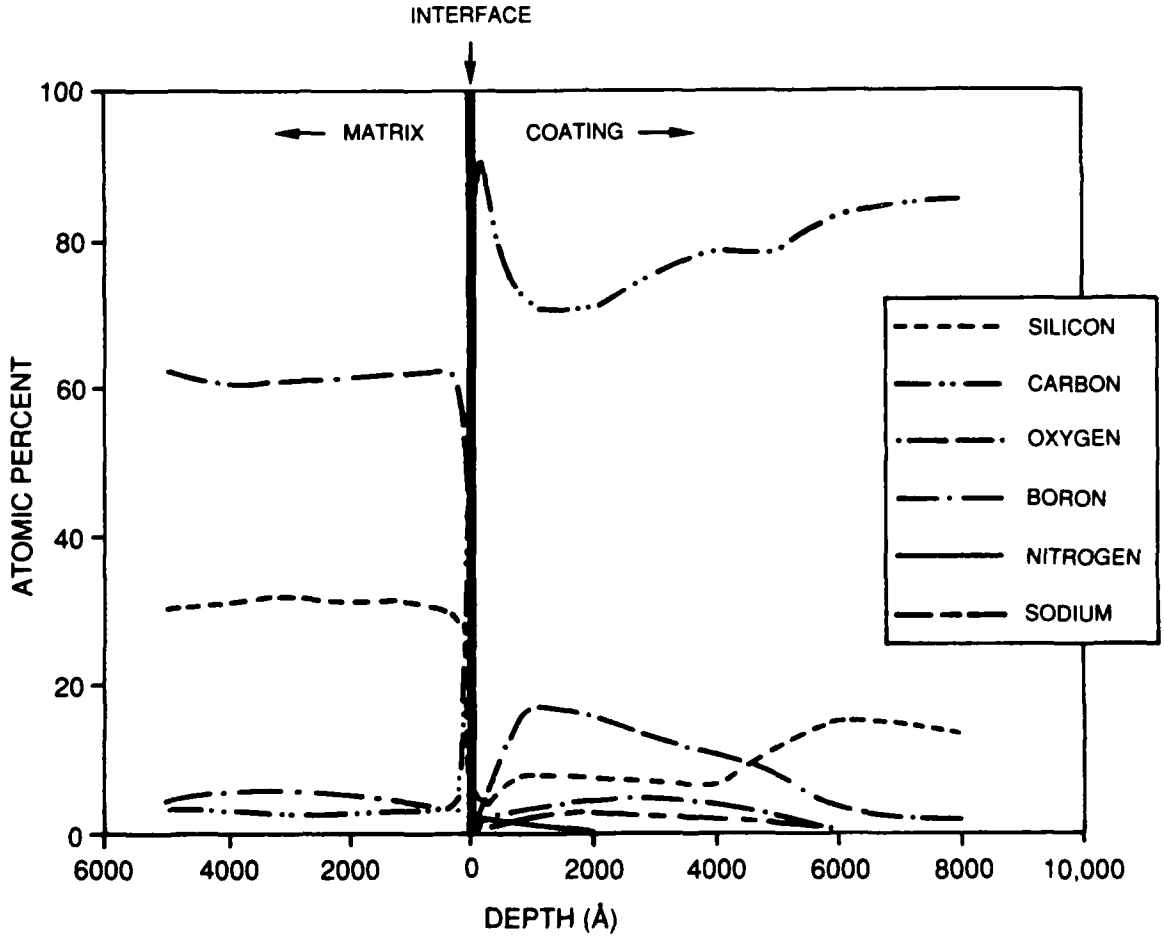


**Figure IV-14 (b). Auger analysis of the coating-matrix interface in a SCS-6/P-100/glass composite.**

90-5-78-3

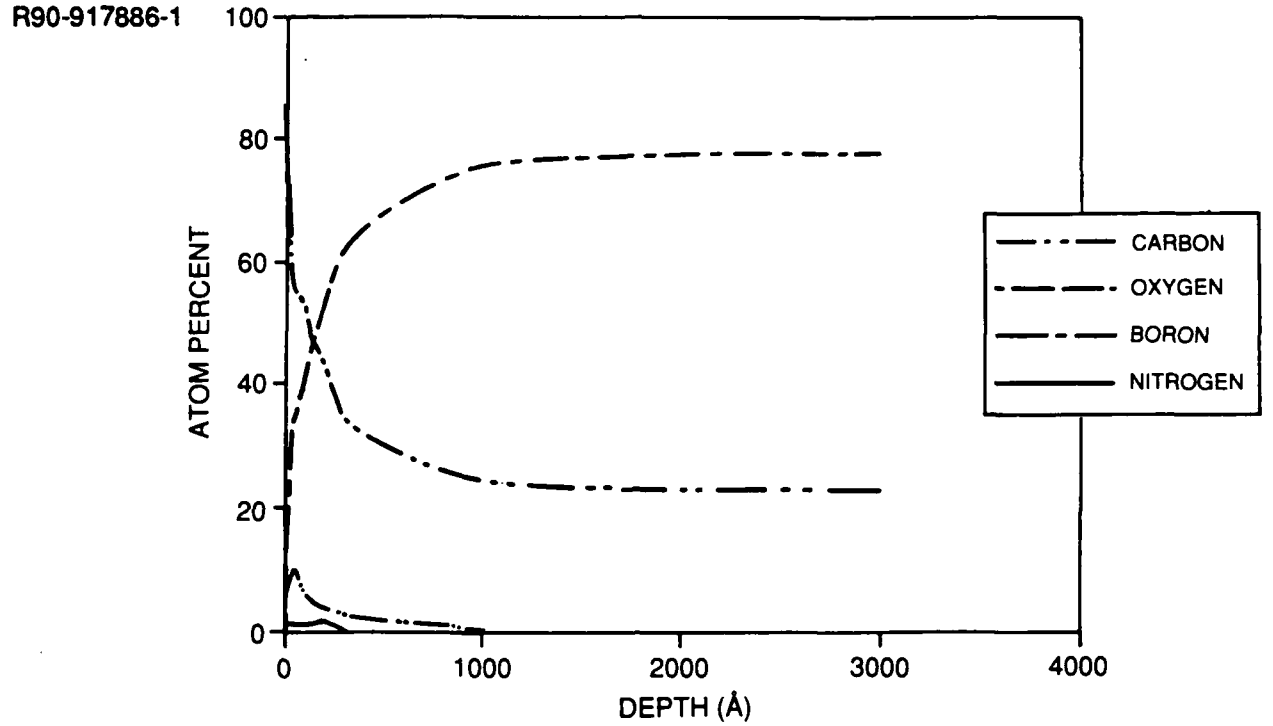


**Figure IV-15 (a). Auger analysis of $B_4C$ coating on $B_4C$-coated boron monofilament.**

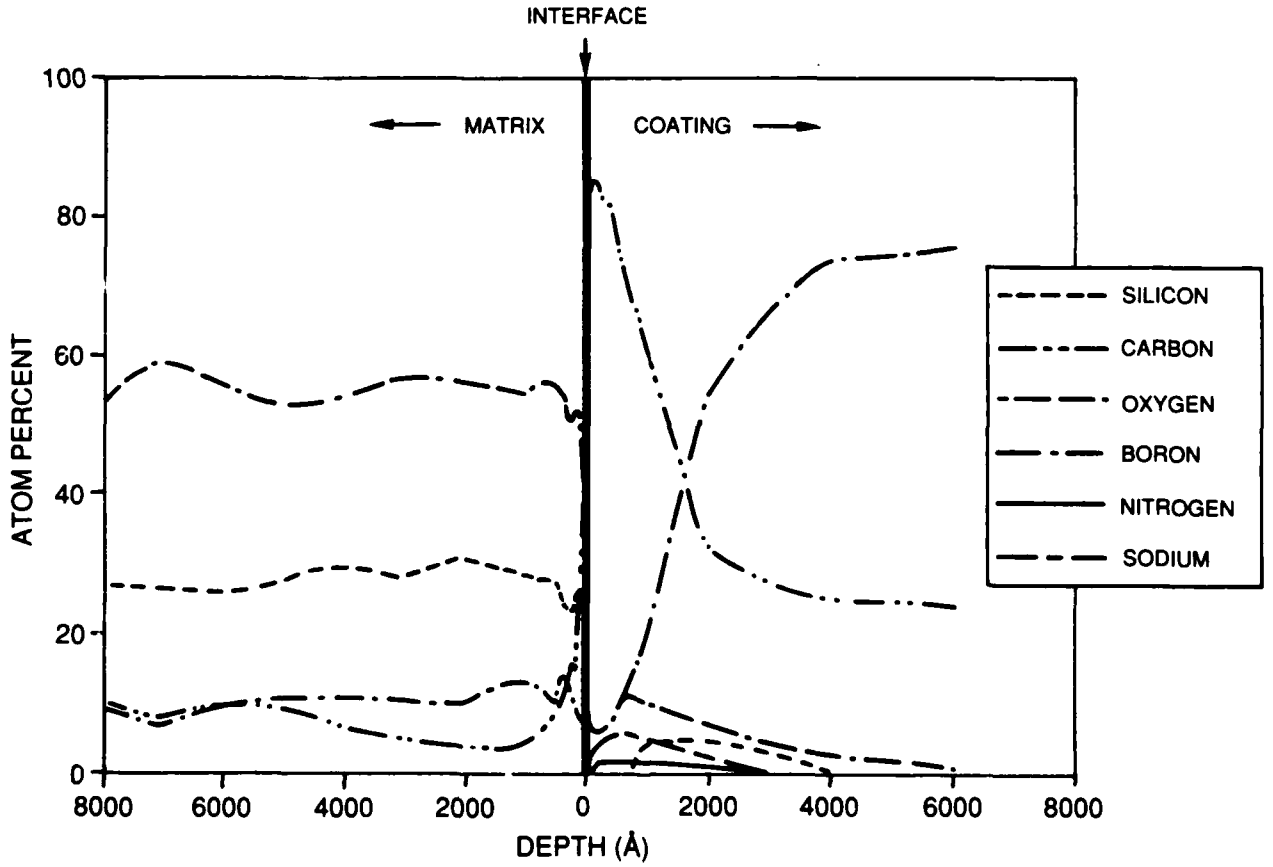


**Figure IV-15 (b). Auger analysis of the coating-matrix interface in a $B_4C$-coated boron/ P-100/ glass composite.**

90-5-78-5

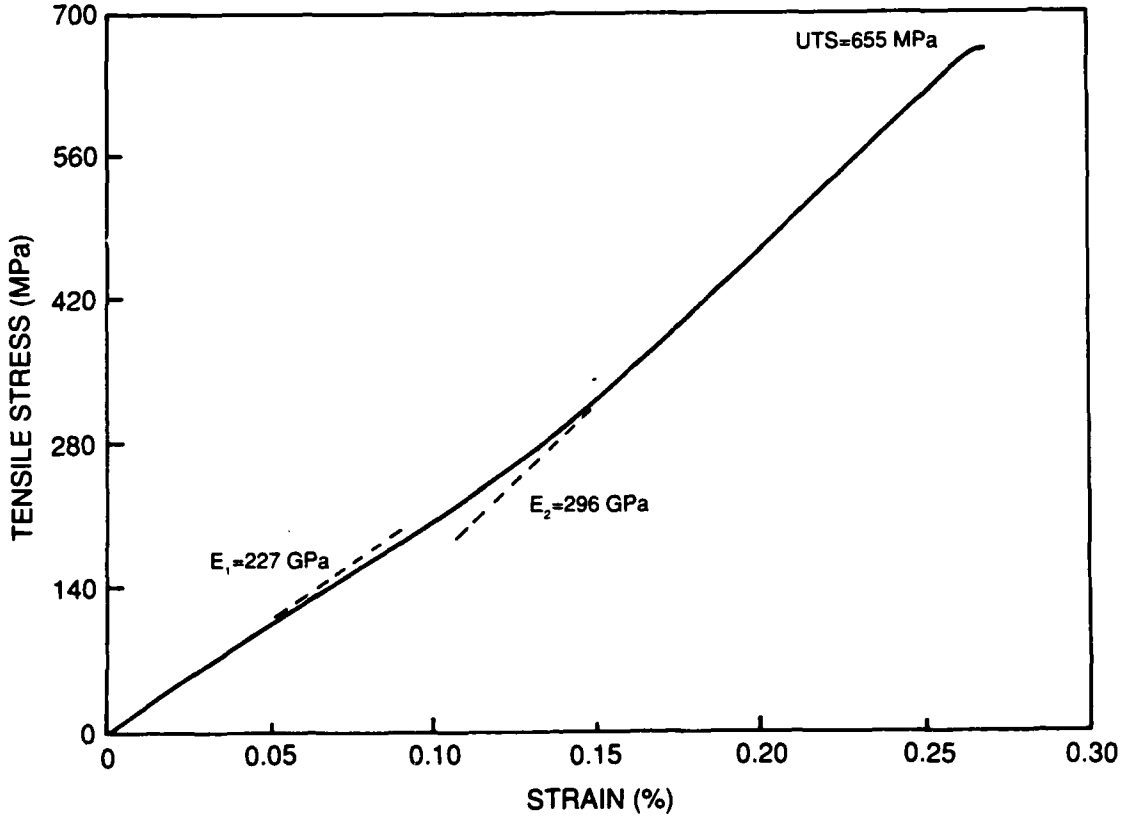


**Figure IV-16. Tensile stress-strain behavior of a uniaxially reinforced SCS-6/P-100/glass composite.**

90-5-78-9

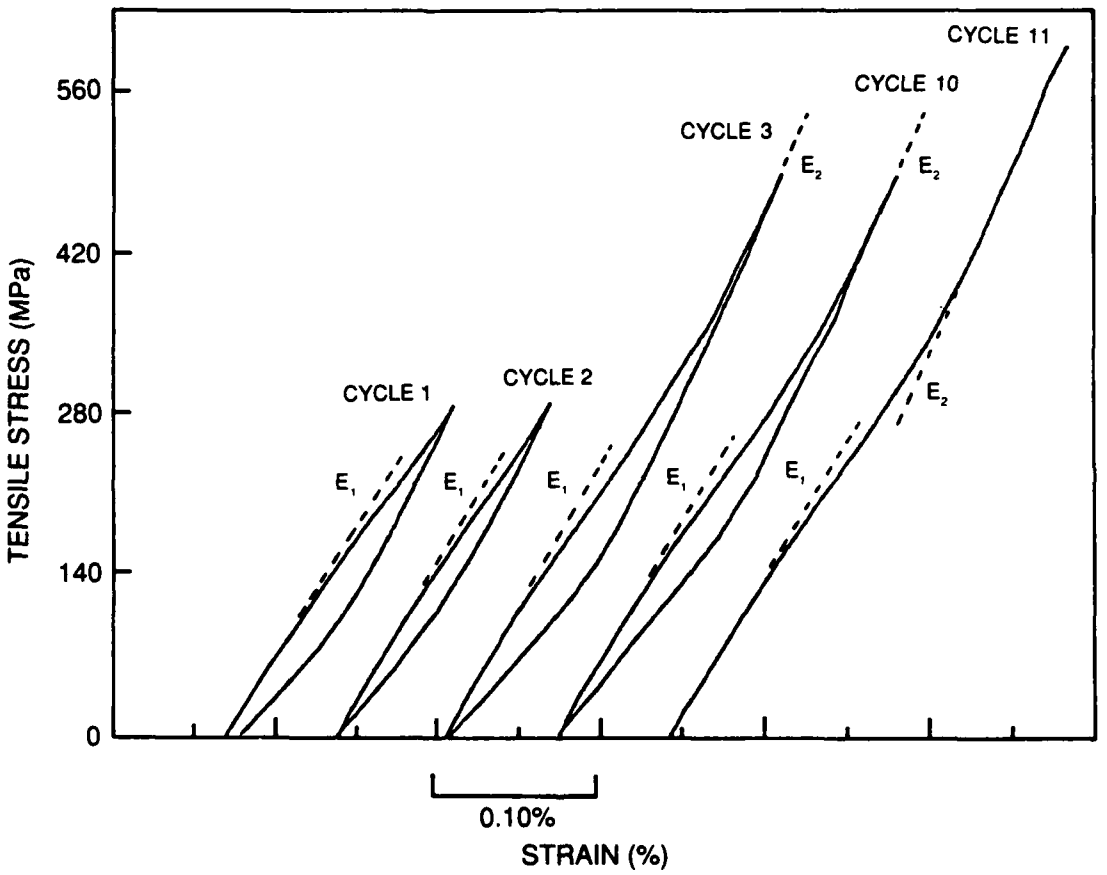


**Figure IV-17. Cyclic tensile stress-strain behavior of a uniaxially reinforced SCS-6/P-100/ glass composite.**

90-5-78-8

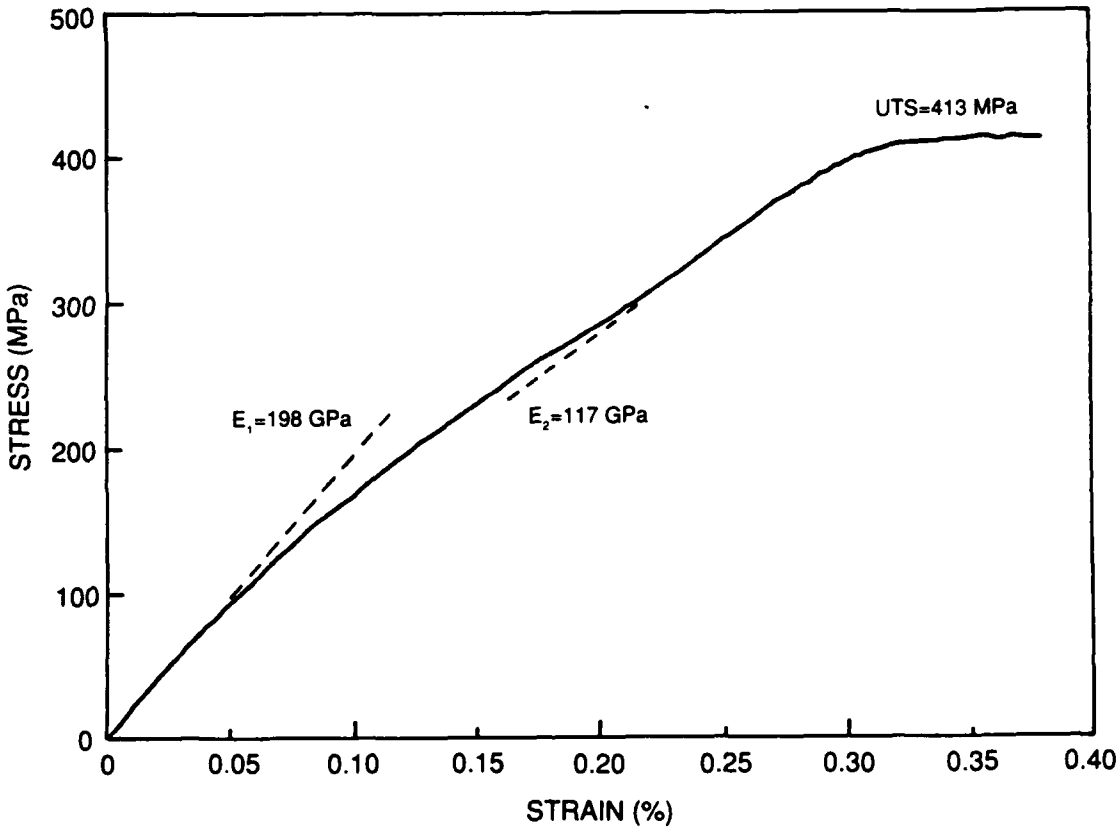


**Figure IV-18. Tensile stress-strain behavior of a uniaxially reinforced Borsic/P-100/glass composite.**

90-5-78-19

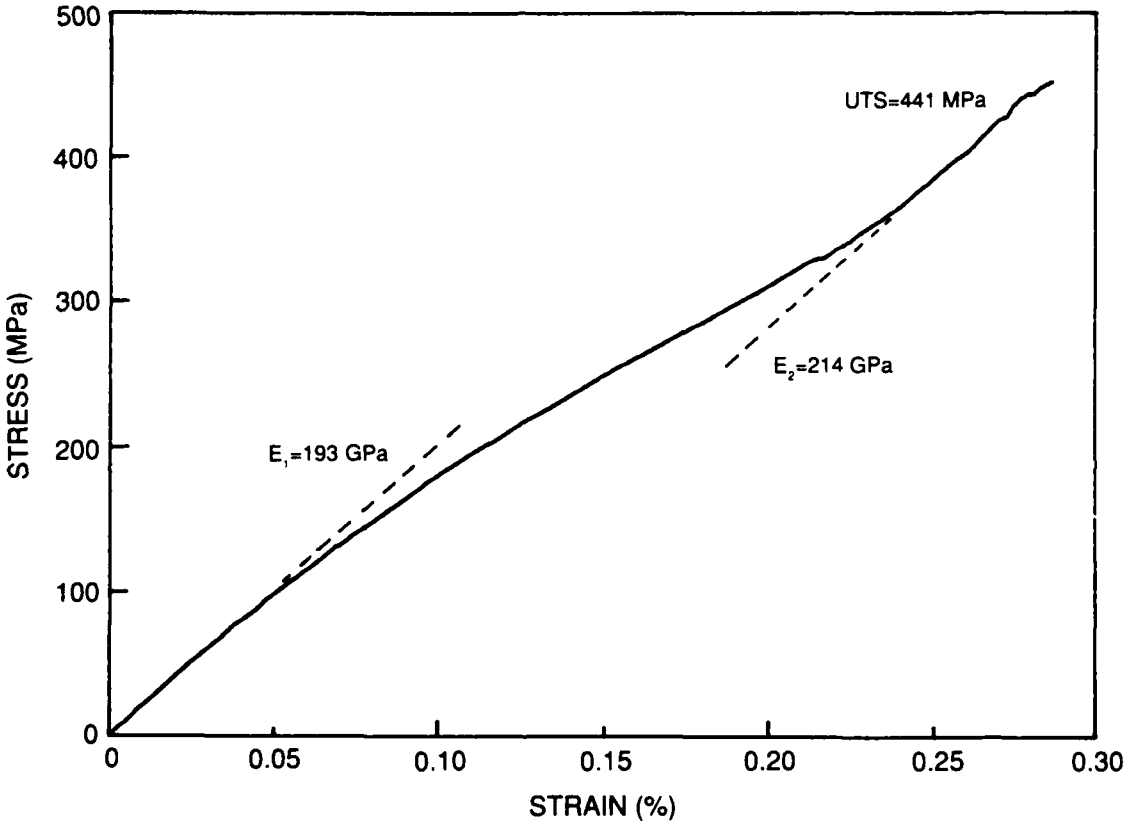


**Figure IV-19. Tensile stress-strain behavior of a uniaxially reinforced Sicabo/P-100/glass composite.**

90-5-78-20

# V. SUMMARY

This program has successfully demonstrated that dual fiber reinforced glass matrix composites can be fabricated using high elastic modulus pitch-based carbon fibers and high stiffness ceramic monofilaments. Specialized tape-making and hot-pressing procedures were used to achieve full density, high strength composites which exhibited unique combinations of properties. This demonstrated capability adds another element of tailorability to these composites for potential space based applications. Following are specific findings of this investigation.

- The concept of tailoring the thermal expansion of a high modulus pitch-based carbon fiber reinforced glass matrix composite to be less negative while maintaining high composite stiffness by adding large diameter monofilaments as a secondary reinforcement to the composite was successful. It was demonstrated that composite thermal expansion could be increased into the near-zero realm over the temperature range of interest (-100°C to +70°C) using a wide variety of monofilaments with and without fiber coatings. For space based applications, structural elements with slightly negative and tailorable CTE are desirable to accommodate the effects of joints and connectors possessing positive CTE.

- A basic understanding of the role of monofilament-matrix interfacial chemistry on composite performance was developed. In the composites containing SCS-6, Borsic, and Sicabo monofilaments, the formation of a carbon-rich layer at the coating-matrix interface during fabrication resulted in weak bonding between the monofilaments and the glass, resulting in extensive monofilament pullout but preventing the monofilaments from contributing fully to the composite elastic modulus. In the composites containing uncoated boron and $B_4C$-coated boron monofilaments, degradation in fiber strength and stiffness occurred during composite fabrication due to diffusion of boron from the fiber into the glass and subsequent void formation at the core-mantle interface.

- The use of coated monofilaments, primarily SCS-6, as the secondary reinforcement for pitch-based carbon fiber reinforced glasses produced composites possessing high tensile strength (up to 655 MPa). However, the unusual stress-strain behavior exhibited by these composites will present unique challenges when designing with these materials for space-based structural elements. For this reason, it would be wise to further pursue the use of boron monofilaments as the secondary reinforcement since composites containing boron monofilament alone have been reported to exhibit good performance [15]. As discussed in the following section (Section VI), it is thought that processing changes may help to improve the performance of dual fiber reinforced composites containing boron monofilaments.

- Table V-1 summarizes the specific stiffness and temperature capability of a number of composites exhibiting near-zero CTE ($\pm$ 0.5 x $10^{-6}$/°C) from -100°C to +100°C. The two metal

matrix composites shown for reference are considered to be very attractive materials for use in space structures. (It is important to note that the properties for the P-100/6061 Aluminum composite are projected properties only; the actual composite itself has never been fabricated due to the very high volume fraction of P-100 fiber that is required to produce near-zero CTE.) It is clear that the dual fiber reinforced composites investigated on this program are competitive with both of the metal matrix composites from the standpoint of specific stiffness. The increased temperature capability resulting from the greater thermal stability of the glass matrix may make these dual fiber reinforced materials an attractive choice for applications requiring a greater degree of survivability. Also included at the bottom of the table are two carbon fiber reinforced glass composites currently being developed on a separate SDIO/ONR funded program at UTRC (ONR contract N00014-89-C-0046). These composites have been fabricated using higher temperature glass and glass-ceramic matrices and exhibit slightly more negative CTE behavior (-1.0 to -0.5 x $10^{-6}$/°C) than the other materials. However, if this can be tolerated, these materials offer specific stiffnesses competitive with the metal matrix composites with an even greater temperature capability than the dual fiber reinforced composites.

**Table V-1 - Potential Composite Materials for Space Applications**

| Fiber | Matrix | Density (g/cc) | Specific Stiffness ($10^7$ cm) | Maximum Temperature Capability (°C) |
|---|---|---|---|---|
| P-100 | 6061 Al | 2.38 | 187 | 300 |
| P-100 | Mg | 1.99 | 178 | 300 |
| Boron | 7740 Glass | 2.24 | 156 | 550 |
| Sicabo/P-100 | " | 2.22 | 88*; 96* | 550 |
| SiC/P-100 | " | 2.32 | 98*; 128* | 550 |
| P-100 | $SiO_2$ Glass | 2.14 | 180 | 800 |
| E-130 | BMAS Glass-ceramic | 2.45 | 169 | 800-1200 |

* Values are for initial and secondary elastic moduli, respectively

# VI. FUTURE ACTIVITY

As stated previously, this study is part of an ongoing activity to prepare glass matrix composites for deployment in space based applications. The following items are planned for future continued investigation to achieve high performance composites.

- Evaluation of the compression behavior of these dual fiber reinforced composites is yet to be determined. It is anticipated that these materials may exhibit considerable compressive strength since the large diameter monofilaments are especially strong in compression. Knowledge of the compression behavior is critical since many space structures are to be loaded primarily in compression.

- Processing parameters for the dual fiber reinforced composites containing boron monofilaments will be altered to retard the diffusion of boron into the glass, which should subsequently reduce degradation at the core-mantle interface and result in fuller retention of monofilament performance. Less diffusion of boron into the glass should also prevent monofilament-matrix interfacial bond strength from being excessively high, which may lead to improved fracture behavior.

- Evaluation of UTRC's newer approach of using coated carbon fibers as a means of controlling composite CTE will be conducted on a separate SDIO/ONR funded program (ONR contract N00014-89-C-0046). Results already obtained on that program indicate that near-zero composite CTE can be readily attained by using BN as a coating for carbon fiber. Other potential coating materials (e.g. SiC) are currently being investigated. This approach is attractive because the fiber coating should provide a combination of improved oxidation resistance together with near-zero composite CTE.

## REFERENCES


1. I. Crivelli-Visconti and G. A. Cooper, "Mechanical Properties of a New Carbon Fiber Material," *Nature*, **221** (1969) 754-755.

2. R. A. J. Sambell, D. H. Bowen and D. C. Phillips, "Carbon Fibre Composites With Ceramic and Glass Matrices - Part 1. Discontinuous Fibres," *J. Mater. Sci.*, **7** (1972) 663-675.

3. D. C. Phillips and A. S. Tetelman, "The Fracture Toughness of Fibre Composites," *Composites*, **3** (1972) 216-223.

4. K. M. Prewo, "Silicon Carbide Yarn Reinforced Glass Matrix Composites," UTRC Internal Report R79-111330-6, October, 1979.

5. K. M. Prewo and J. F. Bacon, "Glass Matrix Composites - I - Graphite Fiber Reinforced Glass," *Proceedings of ICCM/2 - The 1978 International Conference on Composite Materials*, Toronto, Canada, 1978, pp. 64-74.

6. K. M. Prewo, "A Compliant, High Failure Strain, Fibre-Reinforced Glass-Matrix Composite," *J. Mater. Sci.*, **17** (1982) 3549-3563.

7. K. M. Prewo, "Tension and Flexural Strength of Silicon Carbide Fibre-Reinforced Glass Ceramics," *J. Mater. Sci.*, **21** (1986) 3590-3600.

8. J. J. Brennan, "Interfacial Characterization of Glass and Glass-Ceramic Matrix/Nicalon SiC Composites"; pp. 549-560 in *Tailoring Multiphase and Composite Ceramics*. Edited by R. E. Tressler, et al. Plenum Press, New York, 1986.

9. V. C. Nardone and K. M. Prewo, "Tensile Performance of Carbon-Fibre-Reinforced Glass," *J. Mater. Sci.*, **23** (1988) 168-180.

10. K. M. Prewo, B. Johnson and S. Starrett, "Silicon Carbide Fibre-Reinforced Glass-Ceramic Composite Tensile Behaviour at Elevated Temperature," *J. Mater. Sci.*, **24** (1989) 1373-1379.

11. K. M. Prewo, "Carbon Fibre Reinforced Glass Matrix Composite Tension and Flexure Properties," *J. Mater. Sci.*, **23** (1988) 2745-2752.

12. W. K. Tredway and K. M. Prewo, "Carbon Fiber Reinforced Glass Matrix Composites for Structural Space Based Applications," UTRC Report R89-917704-1, ONR Final Report, July 31, 1989.

13. W. K. Tredway, K. M. Prewo and C. G. Pantano, "Fiber-Matrix Interfacial Effects in Carbon Fiber Reinforced Glass Matrix Composites," *Carbon*, **27** (1989) 717-727.

14. V. C. Nardone, et al., "Carbon Fiber Reinforced Metal and Glass Matrix Composites for Space Based Applications," presented at the 19th International SAMPE Technical Conference, Arlington, Virginia, October 13-15, 1987.

15. A. C. Siefert and F. T. Sens, "Fiber Ceramic Composites and Method of Producing Same," U. S. Patent No. 3,575,789, April 20, 1971.

16. D. C. Jarmon and K. M. Prewo, "Characterization of SiC Monofilament Reinforced Glass and Glass-Ceramic Composites," UTRC Report R86-917054-1, ONR Final Report, November 15, 1986.

17. D. C. Jarmon and K. M. Prewo, "SiC Monofilament Reinforced Glass-Ceramic Matrix Composite Properties," *Proceedings of Fiber-Tex '89*, Greenville , South Carolina, 1989.

18. J. Schapery, "Thermal Expansion Coefficients of Composite Materials Based on Energy Principles," *J. Compos. Mater.*, **2** (1968) 380-404.

19. W. K. Tredway and K. M. Prewo, "Mechanical Performance of Pitch Fiber Reinforced Glass Matrix Composites," *To be submitted for publication* (1990).

20. J. A. DiCarlo and T. C. Wagner, "Oxidation-Induced Contraction and Strengthening of Boron Fibers," *Ceram. Eng. and Sci. Proc.*, **2** (1981) 872-893.

21. J. Eason and F. Wawner, "Interfacial Void Formation in Boron Filaments," *J. Mater. Sci.*, **21** (1986) 687.

22. J. DiCarlo, NASA-Lewis Research Center, 1990, personal communication.

23. L. Hwan, S. Suib and F. Galasso, "Silicon Carbide-Coated Boron Fibers," *J. Am. Ceram. Soc.*, **72** (1989) 1259-1261.

24. R. F. Cooper and K. Chyung, "Structure and Chemistry of Fibre-Matrix Interfaces in Silicon Carbide Fibre-Reinforced Glass-Ceramic Composites: An Electron Microscopy Study," *J. Mater. Sci.*, **22** (1987) 3148-3160.

25. J. J. Brennan, "Interfacial Studies of Whisker Reinforced Ceramic Matrix Composites," UTRC Report R89-917894-1, AFOSR Annual Report, May 31, 1989.

# APPENDIX

Table A-1 lists all of the composites fabricated on the program and summarizes their composition, tensile strengths, elastic moduli, and failure strains.

**Table A-1 - Summary of Dual Fiber Reinforced Composite Data**

| Composite Number | Constituent | Volume Percentage | Orient. | Ultimate Tensile Strength (MPa) | Elastic Modulus (GPa) | Failure Strain (%) |
|---|---|---|---|---|---|---|
| 215-87 | Boron | 16.1 | 0° | 343 | 334 | 0.11 |
| | P-100 | 45.2 | 0° | 345 | 349 | 0.10 |
| | Glass | 38.7 | | | | |
| 241-88 | Boron | 26.7 | 0° | 151 | 221 | 0.25 |
| | P-100 | 38.1 | 0° | | | |
| | Glass | 34.1 | | | | |
| 309-88 | Boron | 21.6 | 0° | 268 | 255 | 0.12 |
| | P-100 | 32.8 | 0° | 287 | 245 | 0.13 |
| | Glass | 43.1 | | | | |
| 320-88 | Boron | 18.6 | 0° | 170 | 176 | 0.14 |
| | P-100 | 22.1 | 0° | | | |
| | P-100 | 11.1 | 90° | | | |
| | Glass | 45.1 | | | | |
| 384-88 | Boron | 27.9 | 0° | 227 | 313 | 0.08 |
| | P-100 | 42.7 | 0° | 274 | 318 | 0.10 |
| | Glass | 29.5 | | | | |
| 498-88 | SCS-6 | 19.8 | 0° | 614 | 215 | 0.27 |
| | P-100 | 30.8 | 0° | 654 | 225 | 0.27 |
| | Glass | 46.4 | | | | |
| 558-88 | $B_4C$/Boron | 19.5 | 0° | 185 | 227 | 0.13 |
| | P-100 | 29.4 | 0° | 221 | 225 | 0.13 |
| | Glass | 50 | | | | |
| 582-88 | Borsic | 21.3 | 0° | 369 | 198 | 0.31 |
| | P-100 | 29.1 | 0° | 415 | 198 | 0.38 |
| | Glass | 49.3 | | | | |

| Composite Number | Constituent | Volume Percentage | Orient. | Ultimate Tensile Strength (MPa) | Elastic Modulus (GPa) | Failure Strain (%) |
|---|---|---|---|---|---|---|
| 625-88 | SCS-6 | 19.0 | 0° | 407 | 194 | 0.23 |
| | P-100 | 28.7 | 0° | 472 | 188 | 0.25 |
| | 7070 Glass | 46.3 | | | | |
| 7-89 | Sicabo | 23.2 | 0° | 426 | 208 | 0.28 |
| | P-100 | 30.6 | 0° | 442 | 196 | 0.29 |
| | 7070 Glass | 43.9 | | | | |
| 37-89 | Sicabo | 22.6 | 0° | 521 | 185 | 0.36 |
| | P-100 | 30.1 | 0° | 507 | 198 | 0.32 |
| | Scrim | 0.4 | | | | |
| | 7070 Glass | 46.8 | | | | |